Neurobiology of Learning and Memory 134 (2016) 91–106

Contents lists available at ScienceDirect

Neurobiology of Learning and Memory

journal homepage: www.elsevier.com/locate/ynlme

Hippocampal–medial prefrontal circuit supports memory updating during learning and post-encoding rest

Margaret L. Schlichting [a], Alison R. Preston [a,b,c,*]

[a] Center for Learning and Memory, The University of Texas at Austin, 1 University Station, C7000, Austin, Texas 78712, USA
[b] Department of Psychology, The University of Texas at Austin, 1 University Station, A8000, Austin, TX 78712, USA
[c] Department of Neuroscience, The University of Texas at Austin, 1 University Station, C0920, Austin, TX 78712, USA

ARTICLE INFO

Article history:
Received 27 April 2015
Revised 22 October 2015
Accepted 7 November 2015
Available online 25 November 2015

Keywords:
Hippocampus
Medial prefrontal cortex
Memory integration
Inference
Connectivity
Diffusion-weighted imaging

ABSTRACT

Learning occurs in the context of existing memories. Encountering new information that relates to prior knowledge may trigger integration, whereby established memories are updated to incorporate new content. Here, we provide a critical test of recent theories suggesting hippocampal (HPC) and medial prefrontal (MPFC) involvement in integration, both during and immediately following encoding. Human participants with established memories for a set of initial (AB) associations underwent fMRI scanning during passive rest and encoding of new related (BC) and unrelated (XY) pairs. We show that HPC–MPFC functional coupling during learning was more predictive of trial-by-trial memory for associations related to prior knowledge relative to unrelated associations. Moreover, the degree to which HPC–MPFC functional coupling was enhanced following overlapping encoding was related to memory integration behavior across participants. We observed a dissociation between anterior and posterior MPFC, with integration signatures during post-encoding rest specifically in the posterior subregion. These results highlight the persistence of integration signatures into post-encoding periods, indicating continued processing of interrelated memories during rest. We also interrogated the coherence of white matter tracts to assess the hypothesis that integration behavior would be related to the integrity of the underlying anatomical pathways. Consistent with our predictions, more coherent HPC–MPFC white matter structure was associated with better performance across participants. This HPC–MPFC circuit also interacted with content-sensitive visual cortex during learning and rest, consistent with reinstatement of prior knowledge to enable updating. These results show that the HPC–MPFC circuit supports on- and offline integration of new content into memory.

1. Introduction

Episodic memories do not exist in isolation, but rather influence one another in important ways (Moscovitch et al., 2005; Nadel, Hupbach, Gomez, & Newman-Smith, 2012). For example, new learning events that relate to prior knowledge may trigger reactivation of the existing memory, which may then be modified as a function of the current experience (Gershman, Schapiro, Hupbach, & Norman, 2013; Hupbach, Gomez, Hardt, & Nadel, 2007; Kuhl, Bainbridge, & Chun, 2012; Nader & Einarsson, 2010; Nader, Schafe, & LeDoux, 2000b; Schlichting & Preston, 2014; Zeithamova, Dominick, & Preston, 2012). In addition to allowing for outcomes like memory distortion (Gershman et al., 2013; Hupbach et al., 2007; Loftus, 2005) and deletion (Nader, Schafe, & LeDoux, 2000a), such retrieval may also benefit new learning. By recalling related memories during a new experience, prior knowledge may serve as a foundation that facilities encoding of the new content (Bartlett, 1932), thereby allowing memories to be linked across time. Such integration is thought to underlie the formation of complex knowledge structures like memory networks (Eichenbaum, Dudchenko, Wood, Shapiro, & Tanila, 1999) or schema (Ghosh & Gilboa, 2013; Preston & Eichenbaum, 2013; van Kesteren, Ruiter, Fernández, & Henson, 2012).

Recent theory has implicated hippocampal (HPC)–medial prefrontal (MPFC) interactions in this process, with MPFC guiding HPC encoding and retrieval when new information can be incorporated into existing knowledge (Preston & Eichenbaum, 2013; Schlichting & Preston, 2015; van Kesteren et al., 2012). We hypothesize that this circuit may be similarly engaged during offline periods to promote integration across episodes (Lewis & Durrant, 2011), with integrated memories ultimately stored in

* Corresponding author at: Center for Learning and Memory, The University of Texas at Austin, 1 University Station, C7000, Austin, TX 78712, United States. Fax: +1 (512) 475 8000.
E-mail address: apreston@utexas.edu (A.R. Preston).

http://dx.doi.org/10.1016/j.nlm.2015.11.005
1074-7427/

MPFC (Schlichting, Mumford, & Preston, 2015). While empirical research has broadly demonstrated involvement of HPC and MPFC in memory integration (Tse et al., 2007, 2011; van Kesteren, Fernández, Norris, & Hermans, 2010; Zeithamova, Dominick, et al., 2012), existing reports diverge in their main findings. While some have shown HPC–MPFC connectivity increases during events associated with strong prior knowledge (Tse et al., 2011; Zeithamova, Dominick, et al., 2012), others have observed decreases (van Kesteren, Fernández, et al., 2010), leaving open questions as to how these findings may fit together under a single mechanism. More evidence is needed to inform our understanding of when and how the HPC–MPFC circuit supports encoding.

Here, we seek to fill this gap in understanding by providing a controlled test of theories regarding interregional interactions during integration (Preston & Eichenbaum, 2013; van Kesteren et al., 2012), particularly focusing on HPC and MPFC as our *a priori* regions of interest. We propose that integration through HPC–MPFC communication reduces interference among related memories, facilitating encoding of overlapping experiences. We manipulate the overlap between prior knowledge and new learning on a memory-by-memory basis, allowing for the examination of HPC–MPFC interactions mediating updating of individual events. Moreover, the heterogeneity of MPFC has been underappreciated in prior research on this topic; differences in structural connectivity across MPFC (Ongür & Price, 2000) suggest that its posterior aspects might be particularly important for integration (Nieuwenhuis & Takashima, 2011; Schlichting et al., 2015). We formally test this idea by interrogating neural signatures within subregions of MPFC.

Here, we provide a targeted investigation of HPC and MPFC contributions to integration both across and within individuals, comparing on- and offline neural engagement during periods reflecting memory updating versus simple associative encoding. Behavioral studies in humans have revealed that passive rest following learning promotes memory for individual episodes (Cowan, 2004; Craig, Dewar, Della Sala, & Wolbers, 2015; Dewar, Alber, Butler, Cowan, & Della Sala, 2012; Melton, 1970), perhaps in allowing for the engagement of early consolidation processes (McClelland, McNaughton, & O'Reilly, 1995). Recent work has extended these findings to demonstrate sleep- (Coutanche, Gianessi, Chanales, Willison, & Thompson-Schill, 2013; Ellenbogen, Hu, Payne, Titone, & Walker, 2007) and rest- (Craig, Dewar, Harris, & Della Sala, 2015) related increases in performance on novel judgments spanning multiple experiences, consistent with the idea that offline processing may also facilitate integration (Buckner, 2010). Mechanistically, sleep-based memory reactivation triggered by HPC sharp wave ripples has been hypothesized to enable connections to be formed among co-activated representations, promoting integration (Lewis & Durrant, 2011) in functionally coupled neocortical regions like MPFC (Wierzynski, Lubenov, Gu, & Siapas, 2009). Inspired by such theories, we propose that similar reorganizational processes may occur during awake rest periods immediately following learning via HPC–MPFC interactions. While sharp wave ripples are known to occur predominantly during slow-wave sleep (Diekelmann & Born, 2010), empirical work in rodents and humans suggests that HPC ripples also occur during awake rest following learning (Axmacher, Elger, & Fell, 2008; Buzsaki, Leung, & Vanderwolf, 1983; Cornwell, Overstreet, & Grillon, 2014; Ego-Stengel & Wilson, 2010). While the behavioral significance of such awake-phase events remains unclear (see however Axmacher et al., 2008), it may be the case that like ripples events during sleep, rest-phase ripples also trigger reactivation of prior experience (Foster & Wilson, 2006; Gupta, van der Meer, Touretzky, & Redish, 2010; Karlsson & Frank, 2009; Schlichting & Preston, 2014; Staresina, Alink, Kriegeskorte, & Henson, 2013) and allow for integration across multiple related memories (Craig, Dewar, Harris, et al., 2015) activated simultaneously in the brain. We thus predicted that HPC–MPFC interactions would be enhanced during rest periods following opportunities for memory updating, with the degree of enhancement predicting integration-related behaviors. Furthermore, as behaviors tapping the HPC–MPFC circuit should depend on the integrity of the underlying structural connections, we hypothesized that more coherent white matter tracts connecting these regions would be associated with superior integration.

2. Materials and methods

Data from some portions of this experiment were described in a previous report (Schlichting & Preston, 2014) examining how processes prior to encoding influence new learning. Here, we focus on how the HPC–MPFC circuit is engaged during and immediately following new learning experiences.

2.1. Participants

Participants were as reported previously (Schlichting & Preston, 2014). Forty-eight right-handed volunteers (27 females; ages 20–33, mean ± SEM = 24.6 ± 0.5 years) participated in the experiment. Consent was obtained in accordance with an experimental protocol approved by the Institutional Review Board at the University of Texas at Austin. Participants received monetary compensation for their involvement in the study. Data from a total of 13 participants were excluded for the following reasons: hardware malfunction ($N = 5$), handedness concerns ($N = 1$), and low memory performance ($N = 7$). Low memory performance was defined as either (a) failure to subsequently recall more than 10% of BC and XY associations studied in the scanner ($N = 6$) or (b) failure to reach near-perfect performance on initial AB associations (<80% cued recall accuracy; $N = 1$). Data from the remaining 35 participants were included in all functional analyses (21 females; ages 20–30, 24.1 ± 0.5 years). An additional 10 participants were excluded from the diffusion tensor imaging (DTI) analysis due to data acquisition error. Thus, 25 participants were included in the structural connectivity analysis (15 females; ages 20–30, 24.2 ± 0.7 years).

2.2. Materials

Stimuli for the associative inference task (Fig. 1) (Preston, Shrager, Dudukovic, & Gabrieli, 2004; Zeithamova & Preston, 2010; Zeithamova, Dominick, et al., 2012) consisted of 60 grayscale images of famous faces (30 male and 30 female) and 240 grayscale images of common objects organized into 60 triads (denoted ABC) and 60 pairs (denoted XY). All images were presented with verbal labels. ABC triads consisted of one face and two objects and were presented as overlapping AB and BC pairs, with the B item shared between pairs. That is, AB pairs always consisted of one famous face (A) paired with one object (B) (Fig. 1B); the same object (B) was then paired with a different object (C) to form a BC pair (Fig. 1C, left). Non-overlapping XY pairs consisted of two objects (Fig. 1C, right). All items were unique to their triad or pair, such that a single face or object image was a member of only one ABC triad or one XY pair. Four randomization groups were created to control for the organization of images into triads and pairs and viewing order. Objects were randomly assigned to item type (B, C, X or Y), which determined both whether it belonged to a triad or pair and during which phase(s) it served as a recall cue (see below). An equal number of BC pairs associated with male and female faces (A) were presented within each of two BC encoding scans; no other constraints in item assignment or trial order were imposed. As described below, the order of BC encoding versus XY encoding was counterbalanced across participants.

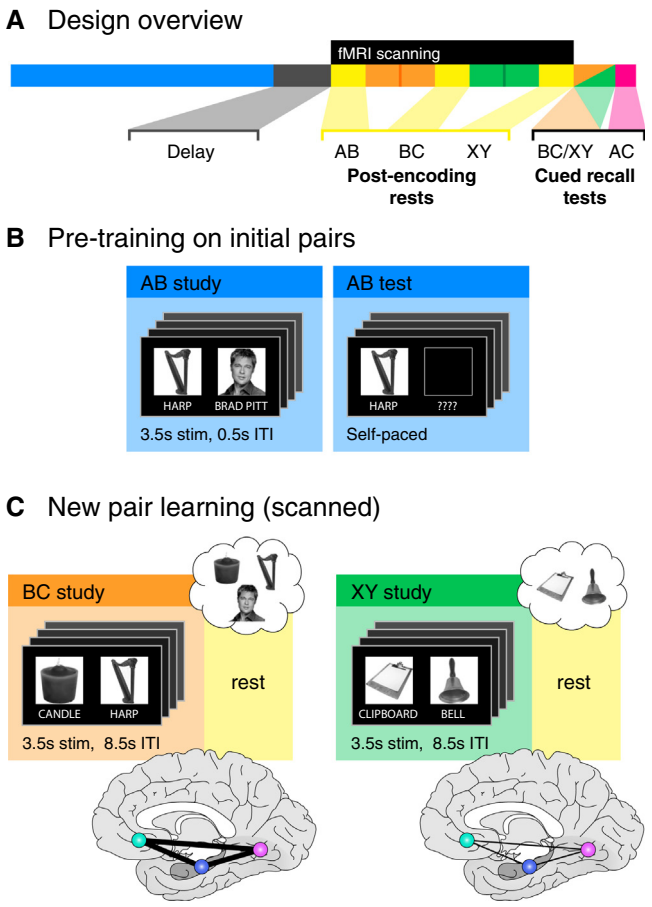

Fig. 1. Experimental design and theoretical predictions. (A) Schematic depiction of the experiment timeline. The present paper focuses on the BC (orange) and XY (green) encoding phases and post-encoding rest periods (yellow). See also panel C. For findings related to the post-AB rest period, see Schlichting and Preston, 2014. (B) Participants learned a series of AB face–object associations across four alternating study-test repetitions during the pre-training phase. Memory performance was near ceiling by the final test block, demonstrating strong memories for the AB pairs (see Results, Behavioral performance). (C) Predictions for the present study. Following the pre-training phase, participants were transferred to the MRI scanner for study of overlapping BC and non-overlapping XY object–object associations. BC and XY study blocks were each followed by a rest period (yellow). The order of BC and XY study was counterbalanced across participants. Left, overlapping BC associations (orange) included one object (here, HARP) that had previously been paired with a face during the pre-training phase (panel A, blue and panel B). Such overlap allows for prior AB memories to be reactivated and updated with the new BC information. We hypothesize that this process engages a network comprising hippocampus (HPC, indigo), medial prefrontal cortex (MPFC, teal), and content-sensitive visual regions (e.g., fusiform face area [FFA], magenta). Right, non-overlapping XY associations (green) included two new objects that had not been previously learned during the pre-training phase. Brain schematics represent the predicted functional connectivity enhancement among HPC, MPFC and FFA for overlapping BC (thick black lines) relative to XY (thin black lines) study and post-encoding rest periods. (For interpretation of the references to color in this figure legend, the reader is referred to the web version of this article.)

2.3. Memory task

An overview of the experimental design is provided in Fig. 1A. Prior to scanning, participants were trained to near-perfect performance on all 60 AB (face–object) pairs (Fig. 1B). The goal of the pre-training phase was to create established memories for the AB pairs, such that overlapping BC information could then be encoded in relation to strong existing memories. The AB pre-training phase consisted of 4 study-test alternations. During the study phase, participants viewed each AB pair once (Fig. 1B, left; 3.5 s stimulus, 0.5 s ITI). A items (faces) were always shown on the right; B items (objects) were always on the left. Participants were encouraged to construct a visual or verbal story linking the items to aid memory but were not required to make any explicit response. Each study phase in the pre-training portion of the experiment lasted 4 min.

Following each study phase, participants completed a self-paced cued recall test (Fig. 1B, right). The B item (object) was presented on the left side of the screen next to an empty box. Participants were asked to say aloud the name of the face that was paired with it. After either a verbal response had been produced or the trial was "passed," participants viewed a feedback display in which the correct image appeared in place of the empty box. Including the feedback displays, each pair was viewed a total of 8 times during the pre-training phase.

After completing the initial AB pair pre-training, participants were transferred to the scanner. At no time were participants made aware by the experimenter of the relationship between the pre-training phase and subsequent study and test tasks (Schlichting & Preston, 2014). Once in the scanner, fMRI data was collected during 6 min of passive rest. During this time, a white fixation cross was displayed on a black screen. Participants were instructed to think about whatever they liked while remaining awake and alert with their eyes open.

Following the initial post-AB rest scan, participants were scanned during encoding of overlapping BC (Fig. 1C, left) and non-overlapping XY pairs (Fig. 1C, right). Pairs were segregated by type into separate scans. There were a total of four slow event-related scans (2 BC scans and 2 XY scans; 3.5 s stimulus, 8.5 s ITI). Participants were encouraged to construct a visual or verbal story while they encoded the new associations; no explicit responses were required. Each pair was presented just once, requiring rapid acquisition of associative information. C and Y objects were on the left; B and X objects were on the right. BC study scans always occurred in immediate succession, as did XY study scans. Encoding order of BC and XY scans was counterbalanced across participants. That is, for half of the participants, all BC pairs (scans 1 and 2) were learned before XY pairs (scans 3 and 4); for the other half, the order was reversed. Each study scan was 6 min long.

Post-encoding rest scans were acquired immediately following BC (e.g., after study scan 2) and XY (e.g., after study scan 4) learning (Fig. 1C, yellow). These scans were identical to the post-AB encoding rest scan described previously. Participants were instructed to think about whatever they liked during the post-encoding rest scans. Importantly, though participants were aware of the overlap between AB and BC associations, they had no reason to believe they would be tested on AC inference associations (in fact, only two participants reported anticipating the AC inference test; see below). Therefore, while explicit rehearsal of the BC or XY pairs is a possibility during these rest scans, it is unlikely that participants would intentionally rehearse the prior related AB knowledge.

After the final rest scan, participants completed a cued recall test on BC and XY pairs (Fig. 1A). This occurred outside of the scanner; no imaging data was collected during the test. C and Y items, presented on the left, served as probes. BC and XY test trials were randomly intermixed. Following completion of the BC/XY test, structure of the inferential (AC) associations was explained to participants. That is, participants were told that A and C items both paired with the same B item were indirectly related. Only two participants reported that they anticipated this inference test, even though all participants became aware of the overlap between the AB and BC associations during the BC study phase. They then completed a cued recall test on these surprise inference associations. The same items (C) served as probes, but this time participants were asked to name the indirectly related item (A, always a face). Importantly, BC and XY associations were of the same content type; they differed only in the degree to which they could be

incorporated into prior (AB) memories. For this reason, we focus primarily on the comparison between BC and XY memory as an index of memory integration; however, we also provide additional follow-up analyses detailing the relationship between neural signatures and subsequent AC performance (notably, AC and BC performance were highly correlated). No feedback was provided during post-scanning BC/XY or AC inference tests to prevent additional learning of the direct (BC/XY) associations.

Participants had the opportunity to practice the memory task before beginning the experiment. The practice included only non-overlapping face–object associations using different stimuli from the main experiment.

2.4. Analysis of behavioral data

Cued recall responses were hand scored. Responses were scored as correct if the participant produced the correct label or, for famous faces, if they provided a unique and accurate description of the person (e.g., by naming a film in which the actor was featured). We used this liberal criterion for recall because we found that participants would often recall a stimulus in great detail despite an inability to remember the specific verbal label. This type of recall performance was true for virtually only the A_{face} stimuli, and was particularly common early in the initial AB pair pretraining. For example, instead of recalling Daniel Radcliffe, the participant may state "the guy who plays Harry Potter." This criterion has been employed in prior studies using a similar stimulus set and paradigm (Kuhl, Rissman, Chun, & Wagner, 2011). A proportion correct was calculated for each participant, pair type (for AB, BC, XY and AC) and repetition (for AB only).

As reported previously (Schlichting & Preston, 2014), performance on BC pairs and AC inferences was highly correlated, both across participants (r_{33} = 0.98) and on a triad-by-triad basis within participant. AB performance also predicted both memory for the overlapping BC information and AC inference performance. For additional behavioral analyses, see Schlichting and Preston (2014).

2.5. Visual localizer task

After the memory task, participants completed a blocked design functional localizer during fMRI scanning to obtain neural patterns associated with viewing different types of visual stimuli. Participants viewed blocks of faces, objects, and scrambled objects while performing a 1-back task. For each image, they pressed one of two buttons on a keypad to indicate whether the picture was new or a repeat of the immediately preceding picture. Responses were collected solely to ensure attention to the task and were not considered as part of the analysis. The images used in the localizer task were different from those used in the memory task. There were four blocks of each stimulus type per run, plus additional interleaved blocks of passive fixation. Blocks were 18 s long, yielding a total run length of 5 min. Three localizer scans were collected.

Participants had the opportunity to practice the visual localizer task before beginning the experiment. The practice contained one abbreviated block of each of the three stimulus types. Practice stimuli comprised images different from those used in the scanned task.

2.6. MR data acquisition

Imaging data were acquired on a 3.0T GE Signa MRI system (GE Medical Systems). All functional data were collected in 33, 3-mm thick oblique axial slices using an EPI sequence (TR = 2000 ms, TE = 30.5 ms, flip angle = 73; 64 × 64 matrix, 3.75 × 3.75 mm in-plane resolution, bottom-up interleaved acquisition, 0.6 mm gap). T2-weighted structural images were acquired in the same prescription as the functional images for the memory (TR = 3200 ms, TE = 68 ms, 512 × 512 matrix, 0.46 × 0.46 mm in-plane resolution) and visual localizer (TR = 3200 ms, TE = 68 ms, 256 × 256 matrix, 0.94 × 0.94 mm in-plane resolution) tasks. Diffusion-weighted data were acquired to characterize white matter structure (TR = 12,000 ms, TE = 87.1 ms, 25 diffusion directions, maximum *b*-value = 1000, 128 × 128 matrix, 0.94 × 0.94 in-plane resolution, 41 straight axial slices, 3-mm thickness, no gap). A T1-weighted 3D SPGR structural volume (256 × 256 × 172 matrix, 1 × 1 × 1.3 mm voxels) was also collected to facilitate image coregistration and for automated parcellation using Freesurfer (http://surfer.nmr.mgh.harvard.edu/) (Desikan et al., 2006).

2.7. fMRI data preprocessing

Functional data were preprocessed using FSL version 5.0.2 (FMRIB's Software Library, http://www.fmrib.ox.ac.uk/fsl). The first 4 volumes of all functional scans were discarded to allow for T1 stabilization. Motion correction was performed within each functional scan using MCFLIRT by aligning all images in the run to the middle volume in the timeseries. Coregistration of functional data across runs was performed by calculating and applying the affine transformation from each run to a reference run using FLIRT, part of FSL. The 3D SPGR structural volume was registered to the functional reference run using the EPI registration utility (part of FLIRT) and then resampled to functional space. Brain extraction was performed on all structural and functional images using BET.

2.8. Regions of interest

2.8.1. Anatomical region of interest definition

The HPC was delineated by hand on the 1 mm MNI template brain and reverse-normalized to each individual's functional space using Advanced Normalization Tools (ANTS) (Avants et al., 2011). Specifically, a non-linear transformation was calculated from the MNI template brain to each participant's 3D SPGR volume. This warp was then concatenated with the SPGR to functional space transformation calculated using FLIRT. After applying the transformation using ANTS, the anatomical HPC ROI was aligned to each participant's functional data.

MPFC ROIs were generated for each participant using output from Freesurfer (Desikan et al., 2006) run on each individual's SPGR. Because previous studies on similar topics (Kumaran, Summerfield, Hassabis, & Maguire, 2009; Sweegers, Takashima, Fernández, & Talamini, 2013; van Kesteren, Rijpkema, Ruiter, & Fernandez, 2010; van Kesteren, Rijpkema, Ruiter, Morris, & Fernández, 2014) have identified a range of activation foci throughout the medial surface of PFC, we combined medial orbitofrontal and rostroanterior cingulate to create an MPFC ROI for each participant. ROIs were then aligned to each individual's functional data using transformations applied in FLIRT, as described above.

2.8.2. Functional region of interest definition

Functional data from the localizer task were used to define face-sensitive voxels within the fusiform gyrus (i.e., fusiform face area, FFA). Analysis of fMRI data from the localizer task was carried out using FEAT (fMRI Expert Analysis Tool) version 6.00, part of FSL. The following pre-statistics processing was applied: grand-mean intensity normalization of the entire 4D dataset by a single multiplicative factor; high-pass temporal filtering (Gaussian-weighted least-squares straight line fitting, with sigma = 64 s); and spatial smoothing (5 mm FWHM). FILM prewhitening was used. Stimulus presentation blocks were modeled as events of 18 s duration, with one regressor for each stimulus type (face, object, scrambled object, passive fixation). Temporal derivates were included. Stimulus regressors were convolved with the canonical (double-gamma)

HRF. Motion parameters calculated during the motion correction step and their temporal derivatives were added as additional confound regressors. Two measures of framewise data quality were also calculated to identify volumes that may be adversely impacted by motion artifacts: framewise displacement (FD) and DVARS (Power, Barnes, Snyder, Schlaggar, & Petersen, 2012). FD measures the overall change in head position from one time point to the next, and is calculated by summing the absolute values of the derivatives of the six motion parameters calculated during the realignment step. DVARS measures the overall change in image intensity from one time point to the next. This index is calculated as the root mean square of the derivatives of the timecourses across all voxels in the brain. Both FD and DVARS were added to the model as regressors of no interest (Schonberg et al., 2014). Additional regressors were created for each time point in which motion exceeded a threshold of both 0.5 mm for FD and 0.5% change in BOLD signal for DVARS (plus one time point before and two time points after) (Power et al., 2012). Temporal filtering was then applied to the model.

After modeling functional data within each run, the resulting statistical images were combined across localizer runs for each participant using fixed effects. As data were already coregistered across runs, no additional registration or spatial normalization was necessary. Face-selective regions were defined for each participant as those voxels responding more to faces than objects and scrambled objects. The procedure for FFA definition was as follows: we created 14 mm spheres centered at each participant's peak voxel (i.e., the maximum *z*-statistic from the face > objects + scrambled objects contrast image) located within the posterior half of their Freesurfer-defined fusiform gyrus. This sphere was then masked with fusiform gyrus to restrict FFA to gray matter voxels. This method was used to ensure FFAs of approximately the same size across participants. This procedure was carried out separately for the left and right hemispheres; lateralized ROIs were then summed to create a bilateral FFA (ROI size range: 205–336 functional voxels, mean ± SEM = 288.7 ± 5.7 voxels). As ROI definition took place in the native functional space of each participant, no realignment or resampling was necessary.

2.9. Univariate analysis

Analysis of fMRI data from the memory task was carried out using FEAT (fMRI Expert Analysis Tool) version 6.00, part of FSL. Grand-mean intensity normalization, high-pass temporal, filtering, spatial smoothing, and pre-whitening were carried out as described above.

We interrogated the relationship between encoding activation and subsequent memory using a general linear model (GLM). The GLM was designed to isolate effects specific to the encoding of new associations that overlapped with prior knowledge. Accordingly, encoding trials were sorted based on both subsequent memory and prior knowledge condition to create four conditions: BC encoding trials that were later correct, BC encoding trials that were later incorrect, XY encoding trials that were later correct, and XY encoding trials that were later incorrect. Contrasts of interest were (1) BC correct > XY correct and (2) BC correct – BC incorrect > XY correct – XY incorrect (i.e., the subsequent recall × prior knowledge interaction).

Stimulus presentations were modeled as events with 3.5 s durations, with one regressor for each condition of interest. The model was convolved with the canonical (double-gamma) HRF. Temporal derivatives were included. Motion parameters calculated during the motion correction step and their temporal derivatives were added as additional regressors of no interest. As described above, FD, DVARS, and individual regressors for time points exceeding FD and DVARS thresholds were added to the models to additionally account for motion effects (Power et al., 2012; Schonberg et al., 2014). Temporal filtering was applied to the model.

After modeling functional data within each run, the resulting statistics images were warped to the MNI template brain resampled to functional resolution (3.75 × 3.75 × 3.6 mm) using ANTS (Avants et al., 2011). The warped images were combined across encoding runs for each participant using fixed effects, and then across the group using mixed effects. For both contrasts of interest, correction for multiple comparisons was carried out at both the whole-brain level and using small volume correction within our *a priori* HPC and MPFC ROIs. Correction for multiple comparisons at the whole-brain level was carried out on group-level voxelwise statistical images according to cluster-based Gaussian random field theory (Worsley et al., 2002), with a cluster-forming threshold of $z > 2.3$ and a whole-brain corrected cluster significance level of $p < 0.05$. We also interrogated activation within *a priori* HPC and MPFC ROIs for integration-specific effects using small volume correction implemented in 3dClustSim, part of AFNI (Cox, 1996). Group statistics images were first masked with each ROI. We then applied a primary voxelwise threshold of $p < 0.05$ to the masked images to identify those voxels within our ROIs surpassing this initial *p*-value threshold. We then corrected for multiple comparisons within the ROIs by determining the cluster extent corresponding to a cluster-corrected threshold of $p < 0.05$ using Monte Carlo simulations. Cluster sizes that occurred with a probability of less than 0.05 across 2000 simulations were considered statistically significant (13 and 19 voxels at functional resolution for HPC and MPFC, respectively).

2.10. Task-based functional connectivity

Functional connectivity during task was examined using a psychological-physiological interactions (PPI; Friston et al., 1997; O'Reilly, Woolrich, Behrens, Smith, & Johansen-Berg, 2012) approach carried out in FEAT version 6.00. Grand-mean intensity normalization, high-pass temporal, filtering, spatial smoothing, and pre-whitening were carried out as described previously.

The PPI analyses were performed to isolate regions whose functional connectivity with HPC and MPFC respectively were significantly modulated by the interaction of subsequent recall by prior knowledge condition. Encoding trials were sorted according to subsequent memory, and a correct – incorrect regressor was constructed for each run. Notably, because BC and XY encoding trials occurred in different scans, this regressor represented the correct – incorrect difference for either BC or XY study trials, depending on the run. This served as the psychological regressor. The first eigenvariate of the filtered timeseries (derived from the univariate analyses described above) was extracted from each individual's anatomically defined HPC and MPFC and functionally defined FFA ROIs and entered as the physiological regressors for the three PPI analyses. The PPI regressor served as the regressor of interest and was generated as the interaction between the psychological and physiological regressors. An additional task regressor was added to account for variance associated with both correct and incorrect trials.

For all three PPI models, stimulus presentations were modeled as events with 3.5 s durations. Task-related regressors and their temporal derivatives were convolved with the canonical (double-gamma) HRF and filtered. Physiological and PPI regressors were not convolved with the HRF or filtered, as these regressors were derived from neural signal that had previously undergone temporal filtering. Motion parameters calculated during the motion correction step and their temporal derivatives were added as additional regressors of no interest. As described above, FD, DVARS, and individual regressors for time points exceeding FD and DVARS

thresholds were added to the models to additionally account for motion effects (Power et al., 2012; Schonberg et al., 2014).

After modeling functional data within each run, the statistics images associated with the PPI regressor were warped to the MNI template brain resampled to functional resolution using ANTS (Avants et al., 2011). The warped PPI images were contrasted for BC and XY study runs for each participant using fixed effects, yielding a subsequent recall × prior knowledge interaction contrast (i.e., BC correct − BC incorrect > XY correct − XY incorrect). These statistics images were then combined across the group using mixed effects. Correction for multiple comparisons was performed within *a priori* HPC and MPFC ROIs using small volume correction implemented in 3dClustSim as described above.

As our anatomical MPFC ROI spans a large and likely functionally diverse region (Ongür & Price, 2000; Price & Drevets, 2009; Roy, Shohamy, & Wager, 2012), we also performed the PPI analysis described above using the MPFC clusters defined in the univariate interaction contrast (depicted in Fig. 2B) as the seed. This analysis was otherwise identical to above.

2.11. Rest-phase functional connectivity

Functional connectivity during rest was interrogated using a voxelwise regression approach with anatomically defined HPC and MPFC and functionally defined FFA as seed regions. This analysis approach is similar to that we have employed previously (Schlichting & Preston, 2014). We interrogated neural activation for clusters of voxels (1) that showed enhanced rest-phase connectivity following overlapping (post-BC) relative to non-overlapping (post-XY) encoding conditions and (2) for which the degree of enhancement was related to subsequent performance. Importantly, we would expect the post-XY rest period to reflect neural signatures related to simple associative encoding (i.e., of object–object pairs), Thus, using this period as a baseline provides a stringent control for isolating those processes related to memory integration above and beyond those engaged during learning more generally.

We first regressed out potential sources of noise from the resting state data. Specifically, we extracted the first eigenvariate of the signal across the duration of the each rest scan in anatomically defined white matter and lateral ventricle ROIs. The signal from these two ROIs and their temporal derivatives were used to construct a GLM along with: motion parameters, FD, DVARS, and their temporal derivatives; and timepoints with excessive motion (as described above). Rest data were high-pass filtered with a cutoff of 0.009 Hz (Fox et al., 2005; Tambini, Ketz, & Davachi, 2010) and regressed on these noise sources. The resulting residual timeseries data for each participant were spatially smoothed (5 mm FWHM).

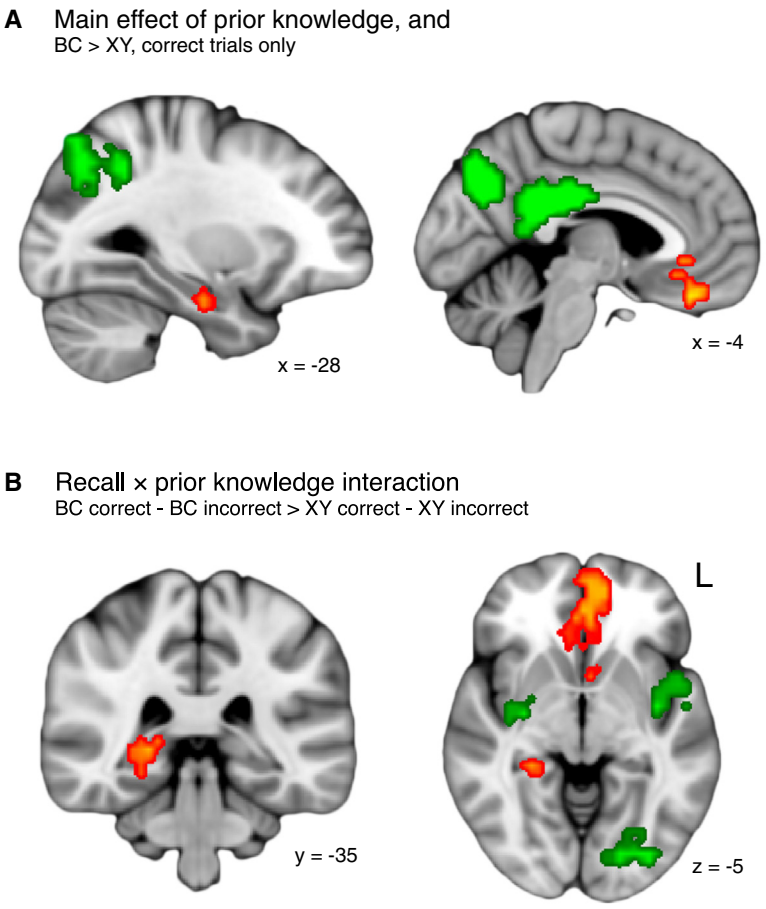

Fig. 2. Activation during overlapping encoding predicts memory updating. Maps include clusters significant at the whole-brain level (green) as well as those that survived correction within *a priori* HPC and MPFC ROIs (orange). (A) Main effect of prior knowledge. Regions in parietal cortex and posterior cingulate survived correction for multiple comparisons across the whole brain. Clusters in both HPC (left) and MPFC (right) showed significantly greater activation during encoding of BC relative to XY pairs (subsequently correct trials only). Clusters are significant after small volume correction within HPC and MPFC, respectively. For all figures, activations were resampled to the 1 mm MNI template for visualization. (B) Interaction of subsequent recall and prior knowledge. Clusters in left fusiform and bilateral insula were significant at the whole brain level. Regions in HPC (left) and MPFC (right) showed a significantly greater subsequent recall effect for BC relative to XY pairs during encoding. Clusters are significant after small volume correction within HPC and MPFC, respectively. Coordinates are in mm. See also Fig. S1 for individual participant data. (For interpretation of the references to color in this figure legend, the reader is referred to the web version of this article.)

As motion-related nuisance signals had already been removed, each model included only the seed ROI timeseries and its temporal derivative. The resulting parameter estimate image for each participant reflected the degree to which activation in each voxel tracked with activation in the seed ROI across each rest scan. We then warped these images to the MNI template resampled to functional dimensions using ANTS (Avants et al., 2011). Images were contrasted within participant (i.e., each participant's post-XY connectivity statistics image was subtracted from their post-BC connectivity image) and combined them across participants using a group-level GLM as follows.

We constructed the group-level model with both BC and XY performance as covariates. To identify those voxels showing enhanced connectivity with the seed region during post-BC relative to post-XY encoding (irrespective of memory performance), we combined the differences images across participants using a one-sample *t*-test. We also isolated voxels for which the degree of connectivity enhancements tracked more with BC than XY performance (i.e., contrast of covariates, BC performance > XY performance; see Schlichting & Preston, 2014). Voxelwise statistics were calculated using permutation tests implemented in Randomise, part of FSL. Correction for multiple comparisons was then performed within *a priori* HPC and MPFC ROIs using small volume correction implemented in 3dClustSim (Cox, 1996) as described above. We also assessed the relationship between connectivity and AC inference performance within the performance-related regions identified above. Contrast values quantifying the degree of connectivity enhancement with the seed region following overlapping BC encoding were extracted and related to AC performance using partial correlation (controlling for XY performance).

As the above analysis searches for regions demonstrating a somewhat complex association with behavior (the difference in post-BC and post-XY connectivity measures relating more to BC than XY performance), it is difficult to know the precise underlying pattern that gives rise to this result. To further describe the results of the above analysis, we extracted post-BC and post-XY connectivity measures separately from significant regions identified above (i.e., showing either an overall connectivity enhancement or an enhancement–performance relationship). These measures were compared across two groups of individuals demonstrating different behavioral signatures: those showing behavior consistent with a facilitative effect of prior knowledge on new learning, and those evidencing proactive interference. We used memory for the non-overlapping XY pairs as a baseline, indexing general memory ability; note that BC and XY pairs are matched in terms of content type (two objects) and number of learning opportunities (one per pair). Thus, differences in memory for these two types of associations must be related to the presence or absence of prior related knowledge. We reasoned that participants who benefitted from prior knowledge during new encoding—who might learn BC pairs by integrating them into prior AB knowledge—would show better memory for the overlapping BC pairs relative to non-overlapping XY pairs (facilitation group; BC performance > XY performance, numeric split; $N = 15$). Other participants, in contrast, might be hindered by the prior AB knowledge, as it interferes with new BC encoding. These participants are expected to show poorer memory for BC relative to XY pairs (interference group; BC performance < XY performance, numeric split; $N = 16$). This analysis excluded individuals who had numerically identical BC and XY performance ($N = 4$). Effects were quantified using 2×2 mixed ANOVAs with rest scan (post-BC or post-XY) as the within-subjects factor and behavioral signature (facilitation or interference) as the between subjects factor *t*-tests. The reader should note that these regions were identified precisely because they showed a significant post-BC enhancement or relationship between enhancement and behavior. Thus, it is not the relationship itself but the nature of that relationship among individuals showing these two behavioral signatures that we sought to isolate.

Due to the large and potentially heterogeneous nature of the anatomical MPFC ROI (Ongür & Price, 2000; Price & Drevets, 2009; Roy et al., 2012), we repeated the main rest-based connectivity analysis described above using the MPFC clusters defined in the interaction contrast (depicted in Fig. 2B) as seed regions.

Additionally, to alleviate the possibility that rest-phase connectivity might be attributed to lingering effects of the task itself, we repeated the analysis omitting the first 30 TRs (60 s) of the rest scan. This analysis lengthened the delay between study and rest connectivity analyses to roughly 3–4 min (in addition to the approximate 2–3 min delay between scans for image reconstruction and communication with the participant).

2.12. Control analyses

As encoding order was counterbalanced across participants, different individuals experienced differences in time (Schlichting & Preston, 2014) and mnemonic demand between initial AB pair pre-training and overlapping BC study. While one group encoded overlapping BC pairs following AB learning, the other encoded non-overlapping XY pairs in between learning AB and BC. One might predict that these differences in encoding order may impact our neural measures of functional activation or interregional connectivity during study and/or post-encoding rest. For instance, one possibility is that the present findings are driven primarily by the group that encoded BC before XY, as the degree to which AB knowledge is brought to bear during BC learning might decrease as AB experience becomes more remote (i.e., temporal proximity of the related experiences may influence these neural mechanisms). Moreover, there may be behavioral differences across groups. Accordingly, we performed additional control analyses to assess the effects of encoding order on our behavioral and neural measures of interest.

2.12.1. Effects of encoding order on behavior

It is possible that the order of encoding overlapping BC versus non-overlapping XY associations might differentially promote memory, as these two groups of participants experienced differences in the relative timing of prior (AB) knowledge formation and related (BC) encoding. We tested whether performance differed as a function of encoding order using a 2×2 mixed ANOVA. Trial type (BC, XY) was the within-subjects factor and encoding order was the between-subjects factor, with performance (proportion correct) serving as the dependent measure. This analysis revealed no significant effect of encoding order (main effect and interaction; both $F < 0.93$, both $p > 0.344$), demonstrating that differences in the relative timing had no significant impact on participants' ability to encode the pairs.

2.12.2. Effects of encoding order at task

We interrogated the encoding phase to determine whether the degree of task-related functional activation or connectivity differed significantly as a function of encoding order. We first focused on clusters showing a significant subsequent recall by prior knowledge condition interaction in univariate activation across the group. We performed a $2 \times 2 \times 2$ mixed ANOVA with subsequent recall and trial type as within-subjects factors and encoding order as the between-subjects factor. Univariate activation served as the dependent measure. We carried out this analysis for all three regions identified in the main analysis as showing a significant interaction effect within our *a priori* regions (two MPFC clusters and one HPC cluster; see Fig. 2). We corrected for multiple comparisons in the three ROIs using Bonferroni correction, which yielded a critical *p*-value of 0.017. Encoding order did not significantly affect

the observed interaction between subsequent recall and prior knowledge condition in any region (main effects and 3-way interactions; all $F_{1,33} < 2.49$, all $p > 0.125$).

We also determined whether task-phase functional connectivity assessed using PPI differed significantly across our counterbalancing groups. We performed a 2 × 2 mixed ANOVA with trial type as the within-subjects factor and encoding order as the between-subjects factor. We note that subsequently correct versus incorrect trials were already contrasted within run; thus, the dependent measures in this analysis reflected the connectivity difference for subsequently correct relative to incorrect trials, separately for BC and XY conditions. This analysis was performed for all six regions identified previously in the main PPI analyses for FFA, HPC, and MPFC seeds (for a total of four HPC clusters and one MPFC cluster; see Fig. 3). Bonferroni correction across the five ROIs yielded a critical p-value of 0.01. We observed no significant effect of encoding order on connectivity measures in any of these regions (main effects and interactions; all $F_{1,33} < 3.27$, all $p > 0.08$).

2.12.3. Effects of encoding order at rest

Next, we investigated the relationship between functional connectivity during rest and encoding order. We first performed a one-way ANOVA to assess whether the degree of connectivity enhancement following BC learning differed as a function of encoding order. Neural measures (degree of connectivity enhancement for post-BC versus post-XY rest) were grouped by encoding order. There was no significant effect of encoding order on the degree of connectivity enhancement ($F_{1,33} = 1.39$, $p = 0.248$).

We performed one-way analyses of covariance (ANCOVA) to determine whether the observed relationships between functional connectivity during rest and performance were related to encoding order. The neural measure served as the independent measure; behavior was the dependent measure. Encoding order was the grouping variable. This analysis was performed for all seven regions identified in the main analyses as relating to performance when FFA, HPC, or MPFC served as the seed region (for a total of five HPC clusters and two MPFC clusters; see Fig. 4). We corrected for multiple comparisons in the seven ROIs using Bonferroni correction, yielding a critical p-value of 0.007. There was no significant effect of encoding order on the observed relationship between connectivity and BC performance controlling for XY performance at our corrected threshold for any region (main effects and interactions; all $F_{1,33} < 5.64$, all $p > 0.024$). We note that the one region in which the interaction effect would be considered significant at a more lenient statistical threshold ($F_{1,33} = 5.64$, $p = 0.024$) was the cluster in left anterior HPC when FFA served as the seed. Interestingly, this interaction was driven by a stronger relationship between connectivity and performance among participants who encoded XY before BC. This is the opposite of what would be predicted by a temporal proximity account, suggesting that our findings are unlikely to reflect merely lingering effects of AB encoding.

2.13. Structural connectivity

DTI data analysis was carried out using tools from FDT (FMRIB's Diffusion Toolbox; Behrens, Berg, Jbabdi, Rushworth, & Woolrich, 2007) version 3.0 and Tract-Based Spatial Statistics (TBSS; Smith et al., 2006), both part of FSL. We were interested in characterizing how white matter structure in pathways connecting HPC and MPFC related to memory for critical BC associations relative to control XY associations. We hypothesized that as the HPC–MPFC circuit supports the updating of existing memories with new information, greater white matter integrity in these tracts should relate to superior overlapping BC pair memory, after accounting for overall differences in memory ability (i.e., performance on non-overlapping XY pairs).

To test this hypothesis, we first isolated tracts connecting anatomical HPC and MPFC ROIs as follows. Registration was carried out within FDT using FLIRT and FNIRT for structural and standard space transformations, respectively. DTI data were first corrected for eddy currents, and then a diffusion tensor model was fit at each voxel of the DTI data for each participant. We generated probability distributions of diffusion parameters at each voxel in the brain for each participant using Bayesian Estimation of Diffusion Parameters Obtained using Sampling Techniques (BEDPOSTX). We then performed tractography between HPC and MPFC ROIs using PROBTRACKX, which uses the voxelwise probability distributions to generate a distribution of pathways connecting specified regions. Probabilistic tractography was carried out for each individual in native DTI space. Each individual's anatomical ROIs were registered to their DTI data using FLIRT transformations computed previously. Tractography was run twice for each participant (number of samples = 5000, curvature threshold = 0.2, maximum number of steps = 2000, step length = 0.5 mm): once from HPC to MPFC (waypoint or inclusion mask); and once from MPFC to HPC. In using this approach, we identified tracts that pass through both ROIs for each individual.

Each individual's HPC–MPFC and MPFC–HPC connectivity distribution maps were thresholded to exclude voxels through which fewer than 5% (250) of all sampled pathways passed. They were then added together to create a single bidirectional white matter ROI for each participant. These white matter ROIs were warped to MNI space using FNIRT transformations computed previously in FDT. ROIs were summed across participants to create a single, group ROI in standard space encompassing all tracts connecting HPC and MPFC. The overlap of white matter ROIs across participants is depicted in Fig. 6A.

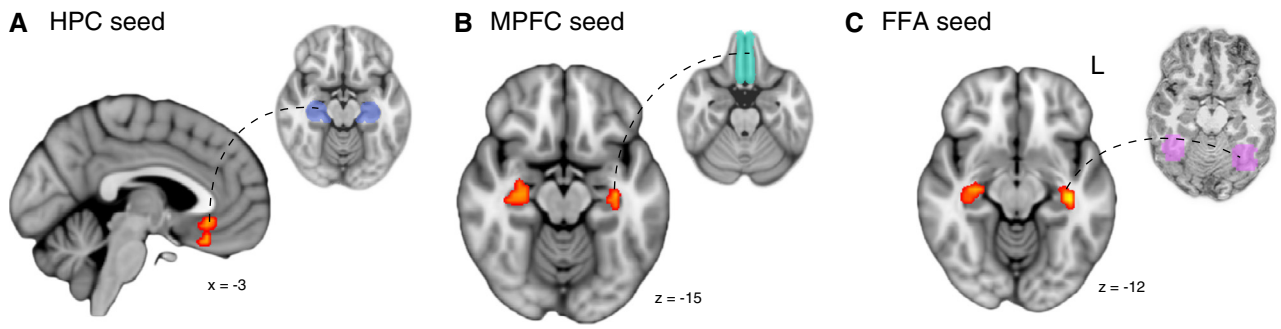

Fig. 3. Functional connectivity during overlapping encoding predicts memory updating. Regions for which functional connectivity with MPFC (A), HPC (B), and FFA (C) showed a significantly greater subsequent recall effect for BC relative to XY pairs during encoding. Clusters are significant after small volume correction within HPC and MPFC. See Fig. S2 for individual participant data.

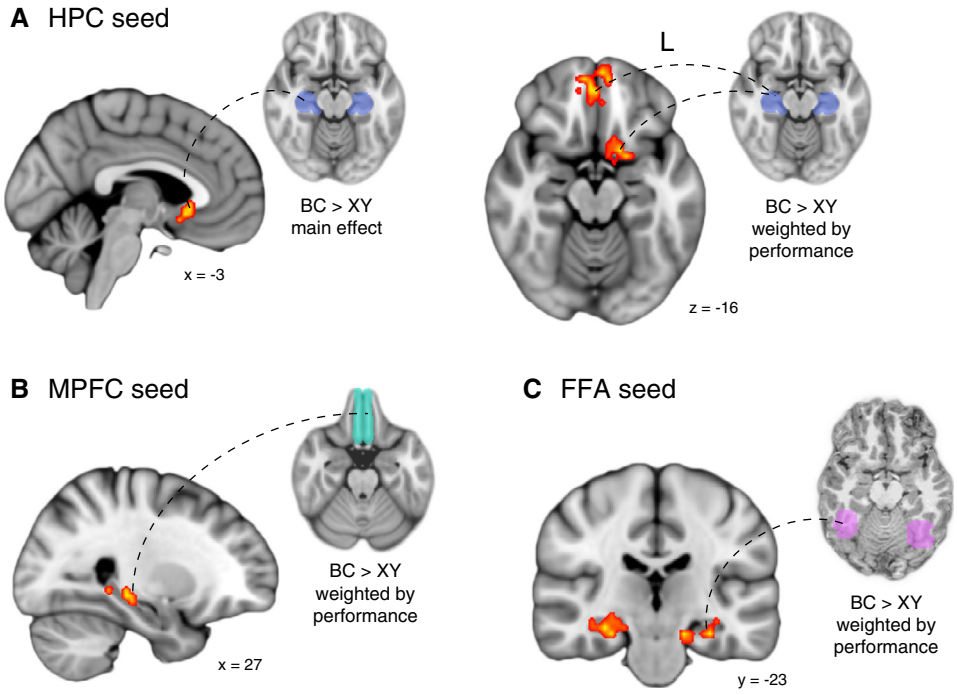

Fig. 4. Functional connectivity enhancements during post-encoding rest tracked integration performance. (A) Left, cluster in MPFC showing greater connectivity with HPC following BC than XY encoding. Right, two clusters in MPFC for which the degree of functional connectivity enhancement with HPC during post-BC encoding rest period tracked more with BC than XY performance across participants. (B) HPC clusters for which enhancement tracked more with BC than XY performance. (C) Functional connectivity with FFA during post-BC encoding rest period tracked more with BC than XY performance across participants in HPC. For all panels, clusters are significant after small volume correction within HPC and MPFC. Coordinates are in mm. See also Fig. 5 for effects split by behavioral signature and Fig. S3 for individual participant data.

Fractional anisotropy (FA) was used as our metric of white matter integrity within this ROI. FA quantifies the degree to which water molecules diffuse in a directional (i.e., anisotropic) manner, and tends to be high when white matter fibers are oriented similarly (i.e., when coherence is high). All subjects' FA data were aligned to common space using FNIRT carried out in TBSS. A mean FA image was then generated and thinned to create a mean FA skeleton, which represents the centers of all tracts common to the group. Each subject's aligned FA data was then skeletonized, i.e., projected onto this group skeleton. Mean FA values were extracted from each individual's skeletonized data across all voxels within the group white matter ROI. FA was related to BC memory and AC inference performance across participants controlling for XY memory using partial correlation (for a similar approach see Schlichting & Preston, 2014).

To assess the specificity of this relationship to HPC–MPFC pathways, we also identified a control white matter ROI, the corticospinal tract, using the Johns Hopkins University (JHU) white-matter tractography atlas (Hua et al., 2008). FA values were then derived from the skeletonized FA data and related to performance measures using partial correlation as described above.

2.14. Stepwise multiple regression

Stepwise multiple linear regression analyses were performed to further assess the degree to which rest-phase functional and structural connectivity measures were independently related to performance. Mean FA values extracted from the HPC–MPFC tract of interest served as the measure of structural connectivity. For functional connectivity, we averaged across the connectivity measures from all four clusters (two HPC, two MPFC; depicted in Fig. 4A, right and Fig. 4B) identified as significantly relating to performance in the rest-phase analyses seeded with HPC or MPFC. Two sets of stepwise regression models were run: one with BC performance as the dependent variable, and one with AC performance as the dependent variable. XY performance, functional connectivity, and structural connectivity measures for each participant were entered into the regression stepwise as predictors. Participants were treated as a random effect.

3. Results

3.1. Behavioral performance

Behavioral performance was as we have published previously (Schlichting & Preston, 2014). Briefly, as intended, AB pairs were well learned by the fourth test block (range: 80–100%, mean ± SEM: 97.3% ± 0.9% correct recall). Importantly, as BC (11.7–86.7%, 41.5% ± 3.3% correct) and XY (10–78.3%, 42.4% ± 3.4% correct) pairs were matched on all dimensions except prior knowledge, we were able to directly compare neural engagement and performance in these two conditions (Fig. 1C). Interestingly, we observed no difference between BC and XY performance across the group ($t_{34} = 0.40$, $p = 0.693$); rather, relative performance on these two conditions was highly variable across individuals (see Schlichting & Preston, 2014 for a more in-depth discussion of the factors modulating the interfering versus facilitative effects of prior knowledge on new learning). This variability enabled us to investigate how neural processes engaged during task and post-encoding rest periods related to performance for overlapping BC relative to control non-overlapping XY pairs. We also found that performance on AC inferences (6.7–83.3%; 41% ± 3.5% correct) paralleled BC memory (Schlichting & Preston, 2014), suggesting that A items were not forgotten over the course of the experiment.

3.2. Hippocampus and medial prefrontal cortex are recruited during encoding of overlapping events

The above framework suggests that HPC and MPFC will be recruited during learning, specifically during episodes in which

interference is reduced through memory updating. We predicted greater activation in these regions during encoding of overlapping BC relative to non-overlapping XY associations. Importantly, we focused on only those associations that were subsequently remembered in both prior knowledge conditions. We searched for this BC correct > XY correct effect both at the whole brain level and within HPC and MPFC regions of interest (ROIs). Two clusters survived correction for multiple comparisons across the whole brain: one in posterior cingulate (−3.75, −39.75, 21.6; cluster extent $k = 230$; all cluster extents reported in functional dimensions, $3.75 \times 3.75 \times 3.6$ mm) and one extending from precuneus on the medial surface to superior parietal lobule (−7.5, −66, 39.6; $k = 608$) (Fig. 2A). Small volume correction revealed significant clusters in both left HPC (−33.75, −13.4, −21.6; $k = 21$) and in MPFC (−3.75, 35.25, −21.6; $k = 49$) (Fig. 2A).

We next assessed the link between encoding activation and subsequent behavior. Our key prediction is that HPC–MPFC engagement and connectivity will be enhanced when new information is successfully integrated into memory. Thus, engagement should be greater for those overlapping BC associations that are later remembered relative to those that are forgotten. Moreover, because BC study events provide the unique opportunity for memory updating via integration, we predicted HPC and MPFC would show a larger subsequent memory effect for BC than XY associations (i.e., a significant interaction between prior knowledge condition and subsequent memory). At the whole brain level, significant clusters were observed in right (41.25, −2.25, 28.75; $k = 74$) and left insula (−37.5, −6, 0; $k = 121$) as well as left fusiform gyrus (−15, −81, −10.75; $k = 138$) (Fig. 2B). We note that due to differences in the spatial normalization approach used between the current study and our previous study (Schlichting & Preston, 2014), the insula regions were not identified in our prior report of this contrast. Using small volume correction, we found one additional significant cluster in right HPC (22.5, −36, 0; $k = 16$) and two in MPFC (anterior: −11.25, 50.25, 0; $k = 131$; posterior: −22.5, 1.5, −14.4; $k = 37$) that showed the predicted interaction (Fig. 2B). Control analyses verified that the observed interaction between subsequent recall and prior knowledge condition did not differ by order of BC versus XY encoding in any region. As our key hypotheses relate to integration-specific neural processes and behavior, all subsequent task-based analyses focus on the prior knowledge condition by subsequent memory interaction.

3.3. Hippocampal–medial prefrontal functional coupling during learning supports memory integration

While the above-described activation results suggest that both HPC and MPFC are engaged during integration, we were also interested in assessing whether their degree of functional coupling would predict subsequent memory for overlapping but not non-overlapping pairs. To examine how functional coupling during new encoding related to the presence or absence of existing knowledge, we performed two psychological–physiological interaction (PPI) analyses with anatomically defined HPC and MPFC, respectively, as seed regions. Using this approach, we were able to test our hypothesis that HPC–MPFC connectivity would be modulated on a trial-by-trial basis as a function of subsequent memory and prior knowledge condition. We predicted greater functional coupling during BC study trials that were later correct relative to those that were incorrect. Moreover, as this effect should be specific to the overlapping study trials, we looked for HPC and MPFC regions that demonstrated this connectivity difference more for BC relative to XY trials.

Consistent with our predictions, we found evidence for recruitment of the HPC–MPFC circuit during successful encoding of overlapping information. We observed significant activation within MPFC (0, 24, −21.6; $k = 26$) when HPC served as the seed (Fig. 3A); and conversely, two significant clusters in HPC (left: −30, −32.25, −7.2; $k = 36$; right: 37.5, −24.75, −7.2; $k = 34$) when MPFC was the seed (Fig. 3B). These effects did not differ significantly by encoding order. Because our anatomical MPFC ROI spanned a large region, we also performed this analysis using the regions identified in the interaction contrast as seeds (i.e., MPFC clusters in Fig. 2B). This analysis yielded similar results (two HPC clusters; left: −33.75, −32.25, −7.2; $k = 38$; right: 33.75, −17.25, −14.4; $k = 43$).

3.4. Encoding-phase functional coupling indicates reinstatement of prior memories in support of updating

A number of existing studies have shown that prior memories may be reactivated during encoding of overlapping experiences (Hupbach et al., 2007; Jones, Bukoski, Nadel, & Fellous, 2012; Kuhl, Shah, DuBrow, & Wagner, 2010; Richter, Chanales, & Kuhl, 2015; Schlichting & Preston, 2014; Zeithamova, Dominick, et al., 2012). Such reactivation has been linked to better memory for the reactivated content itself (Kuhl et al., 2010), superior learning of the overlapping content (Schlichting & Preston, 2014), and an enhanced ability to make novel judgments that span the two events (Richter et al., 2015; Zeithamova, Dominick, et al., 2012). Accordingly, we hypothesized that greater functional coupling of HPC and MPFC with face-sensitive visual regions should also be associated with better subsequent memory specifically for the overlapping associations due to the related A stimuli being faces.

To test this prediction, we performed a PPI analysis with each individual's functionally defined bilateral FFA as the seed region. We found significant clusters in bilateral HPC (left: −37.5, −21, −14.4; $k = 15$; right: 33.75, −17.25, −14.4; $k = 15$; Fig. 3C, left). There were no significant clusters in MPFC. Results did not differ significantly by encoding order.

3.5. Degree of rest-phase hippocampal–medial prefrontal connectivity enhancements predicts memory integration performance

Existing theory suggests that HPC and MPFC interact during sleep to integrate and generalize across discrete experiences (Lewis & Durrant, 2011). Extending these ideas to awake rest periods (Craig, Dewar, Harris, et al., 2015), we hypothesized that greater HPC–MPFC connectivity following overlapping encoding would be associated with more memory updating. We interrogated neural engagement following encoding of the overlapping compared with the non-overlapping associations. We hypothesized that we would observe (1) integration-related enhancements in HPC–MPFC connectivity during post-BC encoding rest relative to post-XY and (2) that the degree of enhancement would relate to behavioral evidence for memory integration across participants.

Using a regression approach, we first searched for voxels in HPC or MPFC for which connectivity with the seed region (MPFC or HPC, respectively) was greater following BC than XY encoding. There were no significant clusters in HPC when MPFC served as the seed. However, when seeding with HPC, we observed a significant region of MPFC that showed the predicted integration-related enhancement (3.75, 16.5, −10.8; $k = 28$; Fig. 4A, left), consistent with the notion that overlapping events trigger a memory updating mechanism.

We also hypothesized that the degree to which participants showed enhanced connectivity following encoding of overlapping relative to non-overlapping associations would correlate with their behavioral evidence for memory integration. That is, if the observed functional connectivity truly reflects integration-specific processes, one would expect that these connectivity enhancements would support performance only for overlapping content. Thus, we identified MPFC and HPC voxels for which

connectivity was more predictive of BC than XY performance. We found two significant clusters in MPFC (anterior: 3.75, 50.25, −14.4; $k = 34$; posterior: −18.75, 5.25, −10.8; $k = 19$) when HPC served as the seed (Fig. 4A, right). We also identified two clusters in HPC (left: −26.25, −28.5, −7.2, $k = 31$; right: 26.25, −28.5, −7.2, $k = 24$) when MPFC served as the seed (Fig. 4B).

We further interrogated the clusters identified as showing the predicted patterns (BC > XY main effect and relationships to performance, depicted in Fig. 4A and B) to determine how connectivity during post-BC and post-XY rest scans related to the different behavioral signatures exhibited across participants. We did this by dividing our group into individuals showing behavior consistent with a facilitative versus interfering effect of prior AB knowledge on BC learning, with XY pairs serving as the baseline. We reasoned that participants for whom prior knowledge was beneficial to new learning would show better memory for the overlapping BC relative to their non-overlapping (baseline) XY pair memory (facilitation group; BC performance > XY performance, numeric split). Conversely, if prior AB knowledge interferes with the learning of new related information, we would expect to see lower memory for BC relative to XY pairs (interference group; BC performance < XY performance, numeric split).

For the MPFC cluster showing enhanced connectivity with HPC for BC versus XY rest across the group (Fig. 4A, left), splitting by behavioral signature revealed that this effect was driven by enhanced connectivity for BC versus XY among participants demonstrating behavioral facilitation (Fig. 5A, top). Interrogating clusters for which the degree of connectivity enhancement tracked with performance across participants, posterior MPFC (Fig. 4A, right) showed a pattern consistent with memory updating only in the facilitation group, with greater connectivity in that group after BC than XY encoding (Fig. 5A, bottom left). Anterior MPFC (Fig. 4A, right) demonstrated a similar connectivity enhancement following BC learning for the facilitation group, but showed the opposite pattern for the interference group; that is, greater connectivity following XY than BC encoding (Fig. 5A, bottom right). HPC regions (Fig. 4B) both showed patterns consistent with integration for the facilitation group (Fig. 5B), albeit weakly in right HPC (Fig. 5B, right).

Control analyses revealed that these effects did not differ significantly as a function of encoding order. To limit the possible effects of the immediately preceding study on rest-phase connectivity, we also performed the above analyses excluding the first minute of the rest scan. This analysis yielded similar results (HPC seed, main effect MPFC cluster: 7.5, 27.75, −14.4; $k = 24$; performance-related MPFC cluster 11.25, 39, −10.8; $k = 30$; MPFC seed, performance-related right HPC cluster: 26.25, −32.25, 0; $k = 29$), suggesting that these findings are unlikely to be the result of continuing study-phase engagement.

We also assessed the across-participant relationship between connectivity enhancements in these regions and AC inference performance. As expected, all regions exhibited significant positive associations with inference performance (partial correlations controlling for XY performance; all $r_{32} > 0.49$, all $p < 0.003$). Moreover, seeding with MPFC regions defined from the univariate interaction contrast instead of the large anatomical MPFC ROI yielded similar clusters in HPC (left: −15, −39.75, 0; $k = 22$; right: 33.75, −32.25, −7.2; $k = 20$). These results are consistent with the prediction that enhanced HPC–MPFC functional coupling following overlapping encoding supports new learning via the integration of that newly learned content into prior related memories.

3.6. Rest-phase connectivity demonstrates offline processing of related memories in support of updating

A number of studies in both rodents and humans have provided evidence that mnemonic content is processed in the brain during offline periods (e.g., rest and sleep) (Deuker et al., 2013; Jadhav, Kemere, German, & Frank, 2012; Staresina et al., 2013; Tambini et al., 2010). For instance, content-specific increases in HPC-neocortical connectivity have been demonstrated following associative encoding (Tambini et al., 2010). Such connectivity enhancements were also related to performance, suggesting that offline processing strengthens memory for recent experiences. We reasoned that immediately following overlapping encoding,

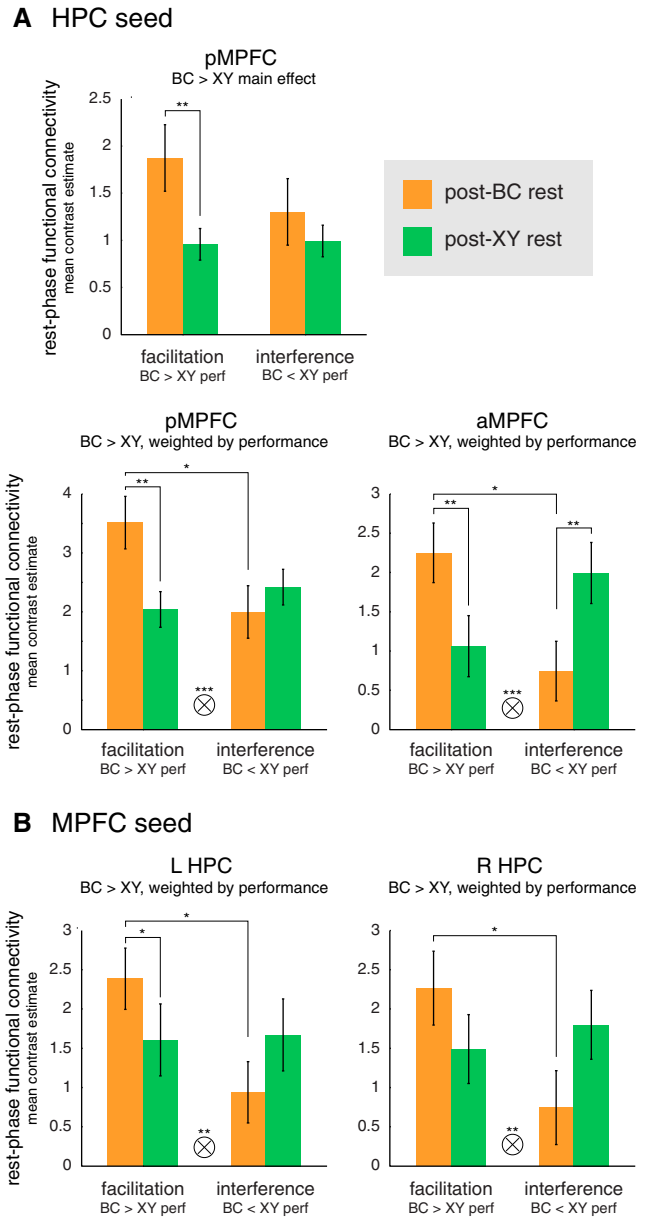

Fig. 5. Rest-phase functional connectivity as a function of rest scan and behavioral signature in clusters demonstrating significant enhancement effects (shown in Fig. 4). Regions were defined using (A) HPC and (B) MPFC seeds for showing either enhanced connectivity during the BC relative to XY rest scan across the group (top chart, cluster depicted in Fig. 4A, left) or a relationship between the degree of BC > XY enhancement and individual differences in performance (bottom four charts, clusters depicted in Fig. 4A, right and Fig. 4B). Connectivity values from the post-BC (orange) and post-XY (green) rest scans were extracted from these clusters and averaged across participants showing facilitation (left bar pairs) and those showing interference (right bar pairs). pMPFC, posterior MPFC; aMPFC, anterior MPFC. Tensor product symbol denotes rest scan by behavioral signature interaction. Asterisks indicate significant level, $^{*}p < 0.05$; $^{**}p < 0.01$; $^{***}p < 0.001$. (For interpretation of the references to color in this figure legend, the reader is referred to the web version of this article.)

HPC and MPFC might show greater connectivity with neocortical regions sensitive to the overlapping content (here, A_{faces}), reflecting persistence of the memory updating process. That is, although participants most recently encoded object–object associations in both BC and XY study phases, we predicted that enhanced functional coupling with face-sensitive regions (FFA) during post-BC relative to post-XY would be associated with superior performance.

Accordingly, we performed a voxelwise regression analysis with FFA serving as the seed region. We found three significant clusters within HPC for which the degree of connectivity enhancement during the post-BC encoding rest period related more to BC than XY performance (Fig. 4C): one in right (30, −21, −14.4; $k = 55$) and two in left (anterior: −11.25, −9.75, −21.6; $k = 14$; posterior: −15, −36, 0; $k = 35$) HPC. Connectivity within these HPC clusters was also significantly related to AC inference performance (partial correlations controlling for XY performance; all $r_{32} > 0.44$, all $p < 0.009$). There were no significant clusters in MPFC. These findings did not differ by encoding order. Similar results were obtained after omitting the first minute of the rest scan (right HPC: 18.75, −24.75, −14.4, $k = 70$; left HPC: −22.5, −39.75, 3.6, $k = 29$; MPFC: 3.75, 5.25, −10.8, $k = 35$).

3.7. White matter integrity predicts performance in tracts connecting HPC and MPFC

The preceding findings indicate that HPC–MPFC activation and functional coupling predicts subsequent memory updating, both during learning on a trial-by-trial basis and during offline periods across participants. We hypothesized that the structural integrity of the white matter tracts connecting these regions would also predict individual differences in the ability to learn overlapping relative to non-overlapping associations. Here, we define white matter integrity as fractional anisotropy (FA), a commonly used measure quantifying the degree to which water molecules diffuse in a directional manner. High FA suggests high white matter integrity or tract coherence. There was no relationship between FA in our control (corticospinal) tract and behavior (i.e., partial correlation with BC and AC performance controlling for XY; BC: $r_{22} = 0.29$, $p = 0.169$; AC: $r_{22} = 0.28$, $p = 0.178$). However, we did find a positive relationship between FA in tracts connecting HPC and MPFC (Fig. 6A) and both BC pair memory and AC inference, after statistically controlling for individual differences in general memory ability (i.e., partial correlation with BC and AC performance controlling for XY; BC: $r_{22} = 0.42$, $p = 0.039$, Fig. 6B; AC: $r_{22} = 0.45$, $p = 0.028$).

3.8. Structural and rest-phase functional HPC–MPFC connectivity independently explain variance in integration performance

To investigate the degree to which HPC–MPFC structural and rest-phase functional connectivity measures independently explained variance in subsequent learning, we next performed two stepwise multiple linear regression analyses with (1) XY performance and indices of (2) structural and (3) rest-phase functional connectivity as independent variables; and BC and AC performance, respectively, as the dependent variables. For both BC and AC performance, the prediction models included all three independent variables. For BC performance, the full model fit was statistically significant ($F_{3,21} = 64.379$, $p < 1 \times 10^{-9}$), accounting for 88.8% of the variance in BC performance (adjusted R^2) and was superior to models with just one (adjusted $R^2 = 0.589$) or two (adjusted $R^2 = 0.862$) predictors. All three independent variables showed a significant positive relationship to BC performance (XY performance: $\beta = 0.92$, $p < 1 \times 10^{-10}$; functional connectivity: $\beta = 0.50$, $p < 1 \times 10^{-6}$; structural connectivity: $\beta = 0.17$, $p = 0.022$; all statistics reflect standardized β), demonstrating the unique contributions of structural and functional HPC–MPFC connectivity to subsequent learning of related experiences. Similar results were found in the stepwise regression model predicting AC performance (full model fit $F_{3,21} = 46.547$, $p < 1 \times 10^{-8}$; adjusted $R^2 = 0.851$, increased from 0.565 and 0.815 with one or two predictors, respectively; XY performance: $\beta = 0.90$, $p < 1 \times 10^{-9}$; functional connectivity: $\beta = 0.48$, $p < 1 \times 10^{-4}$; structural connectivity: $\beta = 0.20$, $p = 0.021$).

4. Discussion

The present study provides convergent evidence from functional and structural MRI methodologies that HPC–MPFC interactions promote integration of new content into existing knowledge, both at the level of individual memories and across participants. This work is consistent with the idea that MPFC resolves competition among memories through integration (Preston & Eichenbaum, 2013) and promotes generalization across episodes (Gilboa et al., 2006; Koscik & Tranel, 2012; Schnider, 2003; Warren, Jones, Duff, & Tranel, 2014). We show that recruitment of the HPC–MPFC circuit benefits new learning, providing a neurobiological account of the age-old observation that knowledge can promote the formation of new, related memories (Bartlett, 1932). Integration-related signatures were observed in posterior MPFC, consistent with this region's proposed role in integrating

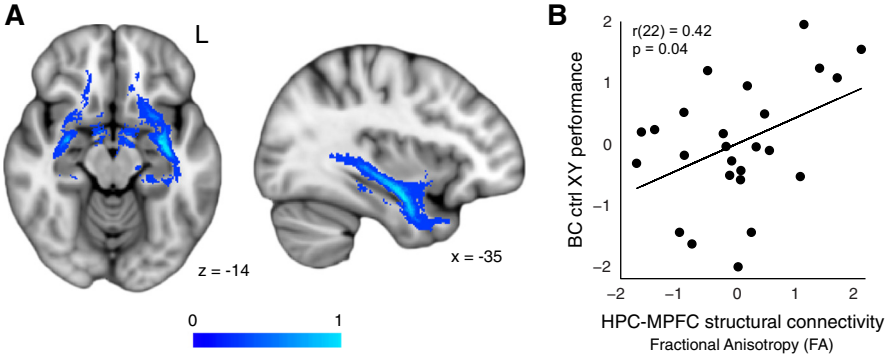

Fig. 6. HPC–MPFC structural connectivity predicts memory updating across participants. (A) Group map depicting overlap across participants of tracts connecting HPC–MPFC. Tracts were determined for each individual using probabilistic tractography, warped to the MNI template and combined across participants. Colorbar indicates the proportion of participants with tracts in each voxel. (B) Mean fractional anisotropy (FA) values were extracted for each participant within the group ROI depicted in panel A. Scatterplot shows across-participant relationship between FA within HPC–MPFC white matter tracts and BC performance, plotted as *z*-scored residuals after regressing both on XY performance.

across inputs (Nieuwenhuis & Takashima, 2011). Structural measures also predicted performance, with greater tract coherence between HPC and MPFC being associated with superior memory integration. We further extend prior human and animal work by showing that content-specific cortical modules interacted with this circuit in service of integration. Specifically, we found that FFA was functionally connected to HPC when new content related to previously learned face–object associations. Despite the large individual differences in behavior in our study, follow-up analyses ensured that our observed effects were not driven by only a few high-performing participants (see Figs. S1–S3).

Enhanced HPC–MPFC coupling when new learning related to prior knowledge was observed not only during intentional study, but also during post-encoding rest periods. Despite the fact that immediately preceding experiences consisted of object–object associations in both cases, functional connectivity and its relationship to memory performance differentiated post-BC from post-XY encoding rest periods. We found that enhanced HPC functional coupling with posterior MPFC following overlapping encoding was associated with behavioral evidence for superior integration. This work extends theories on the sleep-based mechanisms thought to support memory reorganization and integration (Lewis & Durrant, 2011) by providing an empirical test during awake rest. We also observed enhanced HPC functional coupling with FFA during this period, suggesting processing of integrated traces incorporating more remotely encoded but related content (A_{face} items). Taken together, these results suggest a behavioral benefit (Craig, Dewar, Harris, et al., 2015) to offline processing of integrated memories on subsequent recall of the newly learned information.

Theories propose that HPC and MPFC form a highly interactive and dynamic circuit impacting both encoding and retrieval. In particular, MPFC is thought to form memory models (Schacter et al., 2012; St. Jacques, Olm, & Schacter, 2013) that bias HPC retrieval toward task-relevant memories (Kroes & Fernández, 2012; Preston & Eichenbaum, 2013; van Kesteren et al., 2012). When new content overlaps with existing knowledge, MPFC memory models may thus be activated, guiding HPC retrieval of relevant knowledge. HPC encoding mechanisms would then bind current experience to the reactivated content to form integrated memory traces (Preston & Eichenbaum, 2013; Schlichting & Preston, 2015), updating memory models (van Kesteren et al., 2012) through projections to MPFC.

The present findings build upon these theories to provide an understanding of the roles played by subregions of HPC (Giovanello, Schnyer, & Verfaellie, 2009; Poppenk, Evensmoen, Moscovitch, & Nadel, 2013) and MPFC (Nieuwenhuis & Takashima, 2011; Ongür & Price, 2000; Roy et al., 2012; Schlichting et al., 2015) in memory integration. For instance, univariate analyses revealed that activation in posterior HPC predicted subsequent memory for overlapping associations. As previous work has implicated posterior HPC in representing specific event elements (Komorowski, Manns, & Eichenbaum, 2009; Liang, Wagner, & Preston, 2012; Poppenk et al., 2013; Preston & Eichenbaum, 2013; Schlichting et al., 2015), one possibility is that posterior HPC drives retrieval of mnemonic details during new BC encoding.

Notably, in contrast to the univariate activation observed in posterior HPC, task-phase connectivity with MPFC was found more anteriorly. In addition to having direct anatomical projections to MPFC (Barbas & Blatt, 1995), anterior HPC has been implicated in forming generalized representations that span events (Komorowski et al., 2009; Liang et al., 2012; Poppenk et al., 2013; Preston & Eichenbaum, 2013). Thus, one possible interpretation of this finding is that detailed memories reactivated by posterior HPC are communicated to anterior HPC, which in turn integrates and transfers them to MPFC. This interpretation is consistent with recent fMRI work showing integration of related memories in anterior HPC and posterior MPFC (see below; Schlichting et al., 2015), with similar neural representations for indirectly related A and C items formed in these regions. Offline processing of integrated traces may occur through coordinated HPC–MPFC interactions during rest, with reactivation of episodic detail (posterior HPC) and integration across episodes (anterior HPC) occurring simultaneously following overlapping encoding.

In the present study, we observed effects primarily in posterior aspects of MPFC (i.e., subgenual MPFC/anterior cingulate cortex [ACC]) during both encoding and rest. These findings are consistent with work suggesting that this subregion in particular carries out the integrative functions of MPFC (Nieuwenhuis & Takashima, 2011; Roy et al., 2012; Schlichting et al., 2015). Subgenual MPFC exhibits a widespread pattern of anatomical connectivity (Barbas & Blatt, 1995; Cavada, Compañy, Tejedor, Cruz-Rizzolo, & Reinoso-Suárez, 2000; Ongür & Price, 2000), allowing it to integrate across limbic inputs during learning. Damage to this region results in reduced false memory formation (Warren et al., 2014) and poor schema representation (Ghosh, Moscovitch, Melo Colella, & Gilboa, 2014), suggesting its involvement in integrating across sources of information. Engagement of subgenual MPFC also increases with consolidation (Nieuwenhuis & Takashima, 2011), perhaps tracking the increasing importance of abstracted neocortical representations as experiences become more remote. The present work extends these ideas to suggest that enhanced engagement and connectivity of subgenual MPFC with HPC promotes integration of overlapping events into prior memories (Schlichting et al., 2015). The present results may thus reflect both learning-phase biasing of HPC retrieval mechanisms toward relevant memories and rest-phase processing of integrated memories.

We also observed performance-related connectivity of anterior aspects of MPFC (i.e., rostromedial PFC) with HPC during rest. Interestingly, this region showed a different pattern of connectivity than did subgenual MPFC. In anterior MPFC, connectivity was enhanced during post-BC relative to post-XY rest for individuals who showed superior BC relative to XY learning, while the opposite pattern was observed for individuals showing better memory for XY than BC pairs (Fig. 5A, bottom right). One speculative interpretation of this finding is that while subgenual MPFC integrates overlapping content, anterior MPFC performs a more general mnemonic function. Recent work has demonstrated that this region maintains distinct representations of indirectly related A and C items (Schlichting et al., 2015), consistent with the notion that anterior MPFC stores related memories separately. This region has also been implicated in episodic simulation and future thinking (Addis, Pan, Vu, Laiser, & Schacter, 2009; Okuda et al., 2003), which require retrieval and restructuring of episodic details. Thus, one possibility is that during post-encoding rest, anterior MPFC guides reinstatement of both overlapping and non-overlapping associations. Enhanced rest-phase anterior MPFC–HPC connectivity may therefore be associated with superior memory for the preceding pairs, regardless of their relationship to prior knowledge.

Alternate accounts of the present findings might suggest that enhanced HPC connectivity with prefrontal regions during learning reflects other operations such as inhibition (Aron, Robbins, & Poldrack, 2014) or retrieval (King, de Chastelaine, Elward, Wang, & Rugg, 2015; Schedlbauer, Copara, Watrous, & Ekstrom, 2014) of the related A item (without integration). With regards to an interpretation based on inhibition, it is worth noting that such functions have typically been ascribed to right lateral PFC; as such, it is unclear whether MPFC would be expected to perform a similar operation. Moreover, inhibiting the A item during BC encoding would predict forgetting of A's associated with remembered BC pairs due to weakening of the successfully inhibited AB memories.

Our behavioral data are not consistent with this interpretation; rather, BC memory was paralleled by performance on the AC inference test, which required retrieval of the A items. Thus, our findings suggest that AB pair memories were not weakened by BC encoding, which conflicts with an inhibition account.

A second possibility is that HPC–MPFC connectivity reflects retrieval of the A item itself, and not necessarily integration across AB and BC events. Under this hypothesis, MPFC may bias HPC to reinstate the prior memory, but the BC memory is formed separately. We suggest that while such an interpretation is a plausible account of our data, it is important to consider several nuances of how this hypothesis relates to the present analyses. As our task-phase connectivity results index the interaction between trial type and subsequent memory, it must be the case that A item retrieval via HPC–MPFC interactions *promotes* BC encoding. Conflict between prior (AB) retrieved memories and current (BC) experience may be resolved in one of two ways: (1) differentiation, in which the new BC memory is kept distinct from AB (Hulbert & Norman, 2014) or (2) integration of the related AB and BC experiences. We suggest that the particular mechanism reflected in HPC–MPFC connectivity may differ across individuals and across subregions, with both mechanisms (Kumaran, 2012; Schlichting & Preston, 2015; Zeithamova, Schlichting, & Preston, 2012) occurring simultaneously to support inference (Schlichting et al., 2015). As described previously, the present data suggest that while anterior HPC and posterior MPFC may integrate across related memories, posterior HPC and anterior MPFC keep them separate. Interestingly, these results accord with our prior work showing differences in integration and separation of overlapping memories across the anterior–posterior extents of these regions (Schlichting et al., 2015).

Notably, the present findings contrast with a prior study that reported decreased functional coupling for participants with strong prior knowledge (van Kesteren, Fernández, et al., 2010). We propose that there are at least three factors that might account for these discrepancies. First, while the present study trained both initial and overlapping associations within a single day, the previous study (van Kesteren, Fernández, et al., 2010) imposed a 24-h delay between initial learning and overlapping encoding. This difference could have significant implications for memory processes, given the demonstrated importance of sleep for integrating and generalizing across experiences (Buckner, 2010; Lewis & Durrant, 2011). Second, the degree of compatibility between existing knowledge and new experiences—thought to impact integration demands (van Kesteren et al., 2012)—is difficult to compare across paradigms. Prior work (van Kesteren, Fernández, et al., 2010) has theorized that integration demands may be heightened when encoding in the context of incompatible related memories, while our paradigm may encourage resolving incompatibilities via integration precisely when strong prior knowledge exists (Bein, Reggev, & Maril, 2014; Preston & Eichenbaum, 2013; Zeithamova, Dominick, et al., 2012). Third, previous work (van Kesteren, Fernández, et al., 2010) used a large, heterogeneous MPFC ROI to assess connectivity with HPC, thus making it impossible to determine which subregion might have driven their results. Here, we use a voxelwise approach to demonstrate that integration-related connectivity enhancements were found only in posterior MPFC.

We also interrogated white matter structure to find that fractional anisotropy in HPC–MPFC white matter pathways related to memory integration behavior. Prior work (Gerraty, Davidow, Wimmer, Kahn, & Shohamy, 2014) has shown individual differences in resting-state functional connectivity relating to memory integration processes that support generalization. In apparent contrast to the present findings, that study found that intrinsic (i.e., not task-evoked) HPC–MPFC functional connectivity was negatively correlated with behavioral evidence for memory integration (Gerraty et al., 2014). However, HPC and MPFC also showed opposite connectivity–performance relationships with the default mode network (DMN), with low HPC-DMN and high MPFC-DMN connectivity being associated with superior integration. Thus, it is unclear whether the negative relationship between intrinsic HPC–MPFC connectivity and behavior implies more or less reliance on these structures during integration itself. Our results complement this prior report in suggesting that even stable individual differences in structure and function of HPC–MPFC circuitry relate to complex memory behaviors. Importantly, our results rely on an unrelated measure of structural connectivity, highlighting the conceptual convergence across methodologies.

While we focus the present report on our *a priori* HPC and MPFC ROIs, it is notable that a number of regions were more engaged during the encoding of overlapping (BC) relative to non-overlapping (XY) associations in terms of univariate activation at our whole-brain corrected threshold (Fig. 2). Note that these effects are stronger than those in HPC and MPFC, which did not reach significance at the whole-brain level. One possible reason why a more lenient small volume corrected threshold was necessary to reveal the involvement of HPC and MPFC is signal loss in these regions, due to their proximity to air-tissue interfaces. At the whole brain level, clusters in posterior cingulate and precuneus/superior parietal showed greater engagement for subsequently correct BC versus XY encoding trials, perhaps reflecting increased demands on top-down attention (Corbetta & Shulman, 2002; Hutchinson et al., 2014) during overlapping encoding. This could include increased attention to either (a) the BC pair presentation itself, which serves as a retrieval cue for A or (b) the contents of retrieval (i.e., allocating attention to the internal representation of A). We also observed activation in left fusiform gyrus and bilateral insula that was more predictive of subsequent memory for BC than XY associations, consistent with the idea that engaging these regions during learning promoted memory specifically for the pairs overlapping with prior AB knowledge. One interpretation of the fusiform finding is that activation of this region reflects reinstatement of face information during successful encoding of BC pairs (Schlichting & Preston, 2014), which would be required for successful integration. With regards to insula, it is noteworthy that while cognitive operations like switching and conflict resolution have most often been associated with anterior insula (Chang, Yarkoni, Khaw, & Sanfey, 2012; Menon & Uddin, 2010), our clusters spanned both posterior and anterior regions. While we do not have a definitive explanation as to why our task would additionally engage posterior insula, it is noteworthy that this subregion shows the greatest intrinsic functional coupling with ventral MPFC (Chang et al., 2012). Thus, one speculative interpretation of this finding is that engagement of posterior insula reflects its functional relationship to MPFC, with anterior insula additionally aiding in integrating across internal (AB) and external (BC) sources of information (Chang et al., 2012).

5. Conclusions

We demonstrate that fluctuations in HPC–MPFC connectivity track integration demands on a trial-by-trial basis. Our findings also provide novel insight into the timecourse of integration, suggesting the importance of post-encoding rest periods for offline reorganization of overlapping memories. Evidence of rest-phase integration was specific to posterior MPFC, consistent with the notion of dissociable mnemonic functions across MFPC. Moreover, we demonstrate how underlying HPC–MPFC structure relates to integration ability, providing insight into why some individuals are better able to integrate knowledge than others.

Acknowledgments

The authors thank Jackson Liang, Michael Mack, Tammy Tran, Amelia Wattenberger and Dagmar Zeithamova for assistance with data collection and helpful discussions. This work was supported by the National Institute of Mental Health of the National Institutes of Health under award number R01MH100121 and by the National Science Foundation under CAREER award number 1056019 to ARP; and by the Department of Defense (DoD) through the National Defense Science & Engineering Graduate Fellowship (NDSEG) Program to MLS. The authors declare no competing financial interests.

Appendix A. Supplementary material

Supplementary data associated with this article can be found, in the online version, at http://dx.doi.org/10.1016/j.nlm.2015.11.005.

References

Addis, D. R., Pan, L., Vu, M.-A., Laiser, N., & Schacter, D. L. (2009). Constructive episodic simulation of the future and the past: Distinct subsystems of a core brain network mediate imagining and remembering. *Neuropsychologia, 47*, 2222–2238.

Aron, A. R., Robbins, T. W., & Poldrack, R. A. (2014). Inhibition and the right inferior frontal cortex: One decade on. *Trends in Cognitive Sciences, 18*, 177–185.

Avants, B. B., Tustison, N. J., Song, G., Cook, P. A., Klein, A., & Gee, J. C. (2011). A reproducible evaluation of ANTs similarity metric performance in brain image registration. *Neuroimage, 54*, 2033–2044.

Axmacher, N., Elger, C. E., & Fell, J. (2008). Ripples in the medial temporal lobe are relevant for human memory consolidation. *Brain, 131*, 1806–1817.

Barbas, H., & Blatt, G. J. (1995). Topographically specific hippocampal projections target functionally distinct prefrontal areas in the rhesus monkey. *Hippocampus, 5*, 511–533.

Bartlett, F. (1932). *Remembering: A study in experimental and social psychology*. Cambridge: Cambridge University Press.

Behrens, T. E. J., Berg, H. J., Jbabdi, S., Rushworth, M. F. S., & Woolrich, M. W. (2007). Probabilistic diffusion tractography with multiple fibre orientations: What can we gain? *Neuroimage, 34*, 144–155.

Bein, O., Reggev, N., & Maril, A. (2014). Prior knowledge influences on hippocampus and medial prefrontal cortex interactions in subsequent memory. *Neuropsychologia, 64*, 320–330.

Buckner, R. L. (2010). The role of the hippocampus in prediction and imagination. *Annual Review of Psychology, 61*, 27–48.

Buzsaki, G., Leung, L. W. S., & Vanderwolf, C. H. (1983). Cellular bases of hippocampal EEG in the behaving rat. *Brain Research Reviews, 6*, 139–171.

Cavada, C., Compañy, T., Tejedor, J., Cruz-Rizzolo, R. J., & Reinoso-Suárez, F. (2000). The anatomical connections of the macaque monkey orbitofrontal cortex. A review. *Cerebral Cortex, 10*, 220–242.

Chang, L., Yarkoni, T., Khaw, M., & Sanfey, A. (2012). Decoding the role of the insula in human cognition: Functional parcellation and large-scale reverse inference. *Cerebral Cortex*.

Corbetta, M., & Shulman, G. L. (2002). Control of goal-directed and stimulus-driven attention in the brain. *Nature Reviews Neuroscience, 3*, 201–215.

Cornwell, B. R., Overstreet, C., & Grillon, C. (2014). Spontaneous fast gamma activity in the septal hippocampal region correlates with spatial learning in humans. *Behavioural Brain Research, 261*, 258–264.

Coutanche, M. N., Gianessi, C. A., Chanales, A. J. H., Willison, K. W., & Thompson-Schill, S. L. (2013). The role of sleep in forming a memory representation of a two-dimensional space. *Hippocampus, 23*, 1189–1197.

Cowan, N. (2004). Verbal recall in amnesiacs under conditions of diminished retroactive interference. *Brain, 127*, 825–834.

Cox, R. W. (1996). AFNI: Software for analysis and visualization of functional magnetic resonance neuroimages. *Computers and Biomedical Research, 29*, 162–173.

Craig, M., Dewar, M., Della Sala, S., & Wolbers, T. (2015). Rest boosts the long-term retention of spatial associative and temporal order information. *Hippocampus, 1027*, 1–11.

Craig, M., Dewar, M., Harris, M. A., & Della Sala, S. (2015). Wakeful rest promotes the integration of spatial memories into accurate cognitive maps. *Hippocampus*.

Desikan, R. S., Ségonne, F., Fischl, B., Quinn, B. T., Dickerson, B. C., Blacker, D., ... Killiany, R. J. (2006). An automated labeling system for subdividing the human cerebral cortex on MRI scans into gyral based regions of interest. *Neuroimage, 31*, 968–980.

Deuker, L., Olligs, J., Fell, J., Kranz, T. A., Mormann, F., Montag, C., ... Axmacher, N. (2013). Memory consolidation by replay of stimulus-specific neural activity. *Journal of Neuroscience, 33*, 19373–19383.

Dewar, M., Alber, J., Butler, C., Cowan, N., & Della Sala, S. (2012). Brief wakeful resting boosts new memories over the long term. *Psychological Science, 23*, 955–960.

Diekelmann, S., & Born, J. (2010). The memory function of sleep. *Nature Reviews Neuroscience, 11*, 114–126.

Ego-Stengel, V., & Wilson, M. A. (2010). Disruption of ripple-associated hippocampal activity during rest impairs spatial learning in the rat. *Hippocampus, 20*, 1–10.

Eichenbaum, H., Dudchenko, P. A., Wood, E., Shapiro, M., & Tanila, H. (1999). The hippocampus, memory, and place cells: Is it spatial memory or a memory space? *Neuron, 23*, 209–226.

Ellenbogen, J. M., Hu, P. T., Payne, J. D., Titone, D., & Walker, M. P. (2007). Human relational memory requires time and sleep. *Proceedings of the National Academy of Sciences of the United States of America, 104*, 7723–7728.

Foster, D. J., & Wilson, M. A. (2006). Reverse replay of behavioural sequences in hippocampal place cells during the awake state. *Nature, 440*, 680–683.

Fox, M. D., Snyder, A. Z., Vincent, J. L., Corbetta, M., Van Essen, D. C., & Raichle, M. E. (2005). The human brain is intrinsically organized into dynamic, anticorrelated functional networks. *Proceedings of the National Academy of Sciences of the United States of America, 102*, 9673–9678.

Friston, K. J., Buechel, C., Fink, G. R., Morris, J., Rolls, E., & Dolan, R. J. (1997). Psychophysiological and modulatory interactions in neuroimaging. *Neuroimage, 6*, 218–229.

Gerraty, R. T., Davidow, J. Y., Wimmer, G. E., Kahn, I., & Shohamy, D. (2014). Transfer of learning relates to intrinsic connectivity between hippocampus, ventromedial prefrontal cortex, and large-scale networks. *Journal of Neuroscience, 34*, 11297–11303.

Gershman, S. J., Schapiro, A. C., Hupbach, A., & Norman, K. A. (2013). Neural context reinstatement predicts memory misattribution. *Journal of Neuroscience, 33*, 8590–8595.

Ghosh, V. E., & Gilboa, A. (2013). What is a memory schema? A historical perspective on current neuroscience literature. *Neuropsychologia*, 1–11.

Ghosh, V. E., Moscovitch, M., Melo Colella, B., & Gilboa, A. (2014). Schema representation in patients with ventromedial PFC lesions. *Journal of Neuroscience, 34*, 12057–12070.

Gilboa, A., Alain, C., Stuss, D. T., Melo, B., Miller, S., & Moscovitch, M. (2006). Mechanisms of spontaneous confabulations: A strategic retrieval account. *Brain, 129*, 1399–1414.

Giovanello, K. S., Schnyer, D. M., & Verfaellie, M. (2009). Distinct hippocampal regions make unique contributions to relational memory. *Hippocampus, 19*, 111–117.

Gupta, A. S., van der Meer, M. A. A., Touretzky, D. S., & Redish, A. D. (2010). Hippocampal replay is not a simple function of experience. *Neuron, 65*, 695–705.

Hua, K., Zhang, J., Wakana, S., Jiang, H., Li, X., Reich, D. S., ... Mori, S. (2008). Tract probability maps in stereotaxic spaces: Analyses of white matter anatomy and tract-specific quantification. *Neuroimage, 39*, 336–347.

Hulbert, J. C., & Norman, K. A. (2014). Neural differentiation tracks improved recall of competing memories following interleaved study and retrieval practice. *Cerebral Cortex*, 1–15.

Hupbach, A., Gomez, R., Hardt, O., & Nadel, L. (2007). Reconsolidation of episodic memories: A subtle reminder triggers integration of new information. *Learning & Memory, 14*, 47–53.

Hutchinson, J. B., Uncapher, M. R., Weiner, K. S., Bressler, D. W., Silver, M. A., Preston, A. R., & Wagner, A. D. (2014). Functional heterogeneity in posterior parietal cortex across attention and episodic memory retrieval. *Cerebral Cortex, 24*, 49–66.

Jadhav, S. P., Kemere, C., German, P. W., & Frank, L. M. (2012). Awake hippocampal sharp-wave ripples support spatial memory. *Science, 336*, 1454–1457.

Jones, B., Bukoski, E., Nadel, L., & Fellous, J.-M. (2012). Remaking memories: Reconsolidation updates positively motivated spatial memory in rats. *Learning & Memory, 19*, 91–98.

Karlsson, M. P., & Frank, L. M. (2009). Awake replay of remote experiences in the hippocampus. *Nature Neuroscience, 12*, 913–918.

King, D. R., de Chastelaine, M., Elward, R. L., Wang, T. H., & Rugg, M. D. (2015). Recollection-related increases in functional connectivity predict individual differences in memory accuracy. *Journal of Neuroscience, 35*, 1763–1772.

Komorowski, R. W., Manns, J. R., & Eichenbaum, H. (2009). Robust conjunctive item-place coding by hippocampal neurons parallels learning what happens where. *Journal of Neuroscience, 29*, 9918–9929.

Koscik, T. R., & Tranel, D. (2012). The human ventromedial prefrontal cortex is critical for transitive inference. *Journal of Cognitive Neuroscience, 24*, 1191–1204.

Kroes, M. C. W., & Fernández, G. (2012). Dynamic neural systems enable adaptive, flexible memories. *Neuroscience and Biobehavioral Reviews, 36*, 1646–1666.

Kuhl, B. A., Bainbridge, W. A., & Chun, M. M. (2012). Neural reactivation reveals mechanisms for updating memory. *Journal of Neuroscience, 32*, 3453–3461.

Kuhl, B. A., Rissman, J., Chun, M. M., & Wagner, A. D. (2011). Fidelity of neural reactivation reveals competition between memories. *Proceedings of the National Academy of Sciences of the United States of America, 108*, 5903–5908.

Kuhl, B. A., Shah, A. T., DuBrow, S., & Wagner, A. D. (2010). Resistance to forgetting associated with hippocampus-mediated reactivation during new learning. *Nature Neuroscience, 13*, 501–506.

Kumaran, D. (2012). What representations and computations underpin the contribution of the hippocampus to generalization and inference? *Frontiers in Human Neuroscience, 6*, 157.

Kumaran, D., Summerfield, J. J., Hassabis, D., & Maguire, E. A. (2009). Tracking the emergence of conceptual knowledge during human decision making. *Neuron, 63*, 889–901.

Lewis, P. A., & Durrant, S. J. (2011). Overlapping memory replay during sleep builds cognitive schemata. *Trends in Cognitive Sciences, 15*, 343–351.

Liang, J. C., Wagner, A. D., & Preston, A. R. (2012). Content representation in the human medial temporal lobe. *Cerebral Cortex, 23*, 80–96.
Loftus, E. F. (2005). Planting misinformation in the human mind: A 30-year investigation of the malleability of memory. *Learning & Memory, 12*, 361–366.
McClelland, J. L., McNaughton, B. L., & O'Reilly, R. C. (1995). Why there are complementary learning systems in the hippocampus and neocortex: Insights from the successes and failures of connectionist models of learning and memory. *Psychological Review, 102*, 419–457.
Melton, A. W. (1970). The situation with respect to the spacing of repetitions and memory. *Journal of Verbal Learning and Verbal Behavior, 9*, 596–606.
Menon, V., & Uddin, L. Q. (2010). Saliency switching attention and control: A network model of insula function. *Brain Structure and Function*, 1–13.
Moscovitch, M., Rosenbaum, R. S., Gilboa, A., Addis, D. R., Westmacott, R., Grady, C., ... Nadel, L. (2005). Functional neuroanatomy of remote episodic, semantic and spatial memory: A unified account based on multiple trace theory. *Journal of Anatomy, 207*, 35–66.
Nadel, L., Hupbach, A., Gomez, R., & Newman-Smith, K. (2012). Memory formation, consolidation and transformation. *Neuroscience and Biobehavioral Reviews, 36*, 1640–1645.
Nader, K., & Einarsson, E. Ö. (2010). Memory reconsolidation: An update. *Annals of the New York Academy of Sciences, 1191*, 27–41.
Nader, K., Schafe, G. E., & LeDoux, J. E. (2000a). Fear memories require protein synthesis in the amygdala for reconsolidation after retrieval. *Nature, 406*, 722–726.
Nader, K., Schafe, G. E., & LeDoux, J. E. (2000b). The labile nature of consolidation theory. *Nature Reviews Neuroscience, 1*, 216–219.
Nieuwenhuis, I. L. C., & Takashima, A. (2011). The role of the ventromedial prefrontal cortex in memory consolidation. *Behavioural Brain Research, 218*, 325–334.
O'Reilly, J. X., Woolrich, M. W., Behrens, T. E. J., Smith, S. M., & Johansen-Berg, H. (2012). Tools of the trade: Psychophysiological interactions and functional connectivity. *Social Cognitive and Affective Neuroscience, 7*, 604–609.
Okuda, J., Fujii, T., Ohtake, H., Tsukiura, T., Tanji, K., Suzuki, K., ... Yamadori, A. (2003). Thinking of the future and past: The roles of the frontal pole and the medial temporal lobes. *Neuroimage, 19*, 1369–1380.
Ongür, D., & Price, J. L. (2000). The organization of networks within the orbital and medial prefrontal cortex of rats, monkeys and humans. *Cerebral Cortex, 10*, 206–219.
Poppenk, J., Evensmoen, H. R., Moscovitch, M., & Nadel, L. (2013). Long-axis specialization of the human hippocampus. *Trends in Cognitive Sciences, 17*, 230–240.
Power, J. D., Barnes, K. A., Snyder, A. Z., Schlaggar, B. L., & Petersen, S. E. (2012). Spurious but systematic correlations in functional connectivity MRI networks arise from subject motion. *Neuroimage, 59*, 2142–2154.
Preston, A. R., & Eichenbaum, H. (2013). Interplay of hippocampus and prefrontal cortex in memory. *Current Biology, 23*, R764–R773.
Preston, A. R., Shrager, Y., Dudukovic, N., & Gabrieli, J. D. E. (2004). Hippocampal contribution to the novel use of relational information in declarative memory. *Hippocampus, 14*, 148–152.
Price, J. L., & Drevets, W. C. (2009). Neurocircuitry of mood disorders. *Neuropsychopharmacology, 35*, 192–216.
Richter, F. R., Chanales, A. J. H., & Kuhl, B. A. (2015). Predicting the integration of overlapping memories by decoding mnemonic processing states during learning. *Neuroimage*.
Roy, M., Shohamy, D., & Wager, T. D. (2012). Ventromedial prefrontal-subcortical systems and the generation of affective meaning. *Trends in Cognitive Sciences, 16*, 147–156.
Schacter, D. L., Addis, D. R., Hassabis, D., Martin, V. C., Spreng, R. N., & Szpunar, K. K. (2012). The future of memory: Remembering, imagining, and the brain. *Neuron, 76*, 677–694.
Schedlbauer, A. M., Copara, M. S., Watrous, A. J., & Ekstrom, A. D. (2014). Multiple interacting brain areas underlie successful spatiotemporal memory retrieval in humans. *Scientific Reports, 4*, 6431.
Schlichting, M. L., Mumford, J. A., & Preston, A. R. (2015). Learning-related representational changes reveal dissociable integration and separation signatures in the hippocampus and prefrontal cortex. *Nature Communications, 6*, 8151.
Schlichting, M. L., & Preston, A. R. (2014). Memory reactivation during rest supports upcoming learning of related content. *Proceedings of the National Academy of Sciences of the United States of America, 111*, 15845–15850.
Schlichting, M. L., & Preston, A. R. (2015). Memory integration: Neural mechanisms and implications for behavior. *Current Opinion in Behavioral Sciences, 1*, 1–8.
Schnider, A. (2003). Spontaneous confabulation and the adaptation of thought to ongoing reality. *Nature Reviews Neuroscience, 4*, 662–671.
Schonberg, T., Bakkour, A., Hover, A. M., Mumford, J. A., Nagar, L., Perez, J., & Poldrack, R. A. (2014). Changing value through cued approach: An automatic mechanism of behavior change. *Nature Neuroscience, 17*, 625–630.
Smith, S. M., Jenkinson, M., Johansen-Berg, H., Rueckert, D., Nichols, T. E., Mackay, C. E., ... Behrens, T. E. J. (2006). Tract-based spatial statistics: Voxelwise analysis of multi-subject diffusion data. *Neuroimage, 31*, 1487–1505.
St. Jacques, P. L., Olm, C., & Schacter, D. L. (2013). Neural mechanisms of reactivation-induced updating that enhance and distort memory. *Proceedings of the National Academy of Sciences of the United States of America, 110*, 19671–19678.
Staresina, B. P., Alink, A., Kriegeskorte, N., & Henson, R. N. (2013). Awake reactivation predicts memory in humans. *Proceedings of the National Academy of Sciences of the United States of America, 110*, 21159–21164.
Sweegers, C. C. G., Takashima, A., Fernández, G., & Talamini, L. M. (2013). Neural mechanisms supporting the extraction of general knowledge across episodic memories. *Neuroimage, 87*, 138–146.
Tambini, A., Ketz, N., & Davachi, L. (2010). Enhanced brain correlations during rest are related to memory for recent experiences. *Neuron, 65*, 280–290.
Tse, D., Langston, R. F., Kakeyama, M., Bethus, I., Spooner, P. A., Wood, E. R., ... Morris, R. G. M. (2007). Schemas and memory consolidation. *Science, 316*, 76–82.
Tse, D., Takeuchi, T., Kakeyama, M., Kajii, Y., Okuno, H., Tohyama, C., ... Morris, R. G. M. (2011). Schema-dependent gene activation and memory encoding in neocortex. *Science, 333*, 891–895.
van Kesteren, M. T. R., Fernández, G., Norris, D. G., & Hermans, E. J. (2010). Persistent schema-dependent hippocampal-neocortical connectivity during memory encoding and postencoding rest in humans. *Proceedings of the National Academy of Sciences of the United States of America, 107*, 7550–7555.
van Kesteren, M. T. R., Rijpkema, M., Ruiter, D. J., & Fernandez, G. (2010). Retrieval of associative information congruent with prior knowledge is related to increased medial prefrontal activity and connectivity. *Journal of Neuroscience, 30*, 15888–15894.
van Kesteren, M. T. R., Rijpkema, M., Ruiter, D. J., Morris, R. G. M., & Fernández, G. (2014). Building on prior knowledge: Schema-dependent encoding processes relate to academic performance. *Journal of Cognitive Neuroscience, 26*, 2250–2261.
van Kesteren, M. T. R., Ruiter, D. J., Fernández, G., & Henson, R. N. (2012). How schema and novelty augment memory formation. *Trends in Neurosciences, 35*, 211–219.
Warren, D. E., Jones, S. H., Duff, M. C., & Tranel, D. (2014). False recall is reduced by damage to the ventromedial prefrontal cortex: Implications for understanding the neural correlates of schematic memory. *Journal of Neuroscience, 34*, 7677–7682.
Wierzynski, C. M., Lubenov, E. V., Gu, M., & Siapas, A. G. (2009). State-dependent spike-timing relationships between hippocampal and prefrontal circuits during sleep. *Neuron, 61*, 587–596.
Worsley, K. J., Liao, C. H., Aston, J., Petre, V., Duncan, G. H., Morales, F., & Evans, A. C. (2002). A general statistical analysis for fMRI data. *Neuroimage, 15*, 1–15.
Zeithamova, D., Dominick, A. L., & Preston, A. R. (2012). Hippocampal and ventral medial prefrontal activation during retrieval-mediated learning supports novel inference. *Neuron, 75*, 168–179.
Zeithamova, D., & Preston, A. R. (2010). Flexible memories: Differential roles for medial temporal lobe and prefrontal cortex in cross-episode binding. *Journal of Neuroscience, 30*, 14676–14684.
Zeithamova, D., Schlichting, M. L., & Preston, A. R. (2012). The hippocampus and inferential reasoning: Building memories to navigate future decisions. *Frontiers in Human Neuroscience, 6*, 70.